

RBM

H. O. Misc. 15360

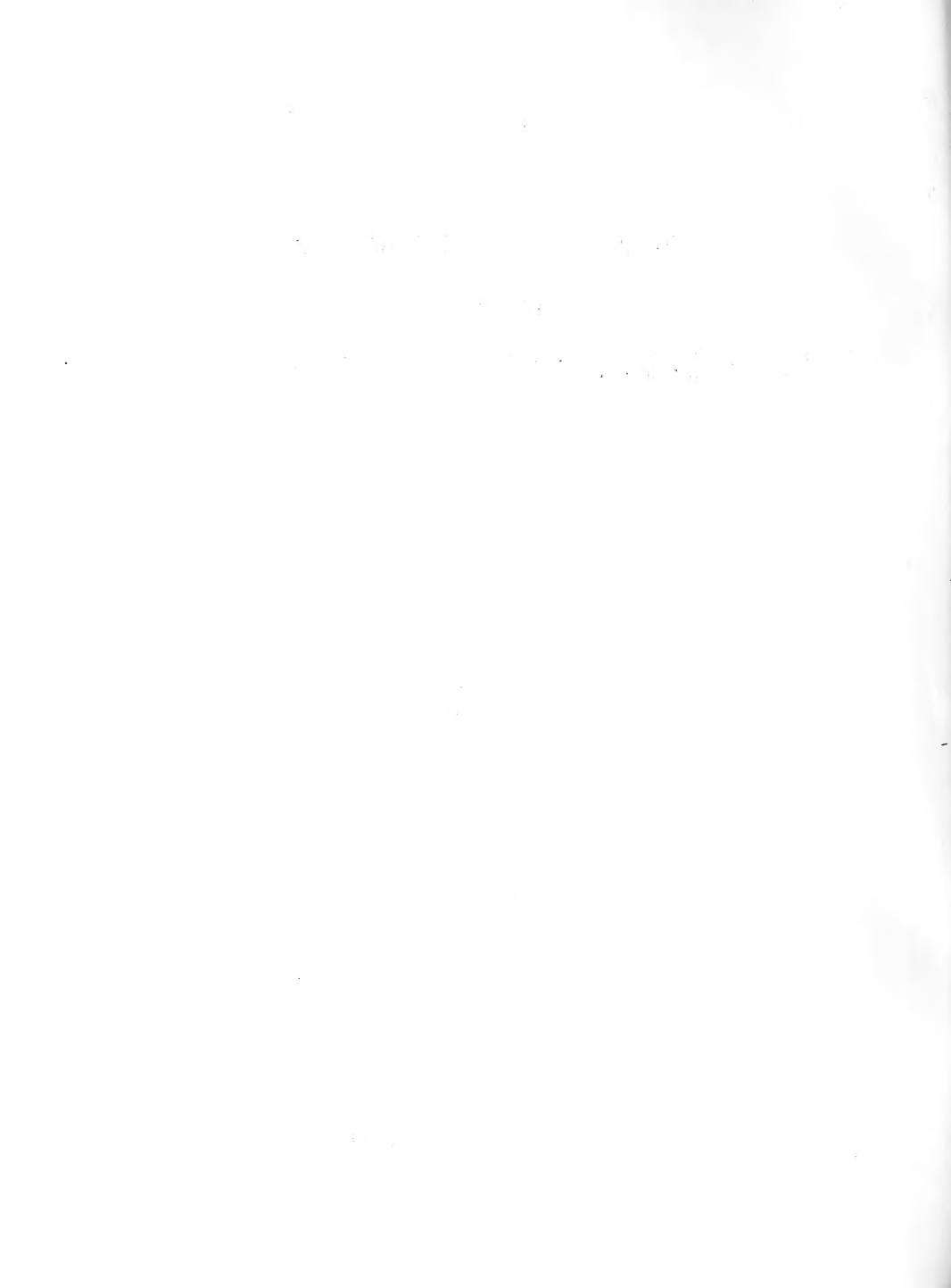
EFFECTS OF WEATHER
UPON THE
THERMAL STRUCTURE OF THE OCEAN

Woods Hole Oceanographic Institution
ATLAS GAZETTEER COLLECTION



U. S. NAVY HYDROGRAPHIC OFFICE
WASHINGTON, D. C.

GC
161
S88
1952



H. O. Misc. 15360

GC
161
588
1952

EFFECTS OF WEATHER UPON THE THERMAL STRUCTURE OF THE OCEAN

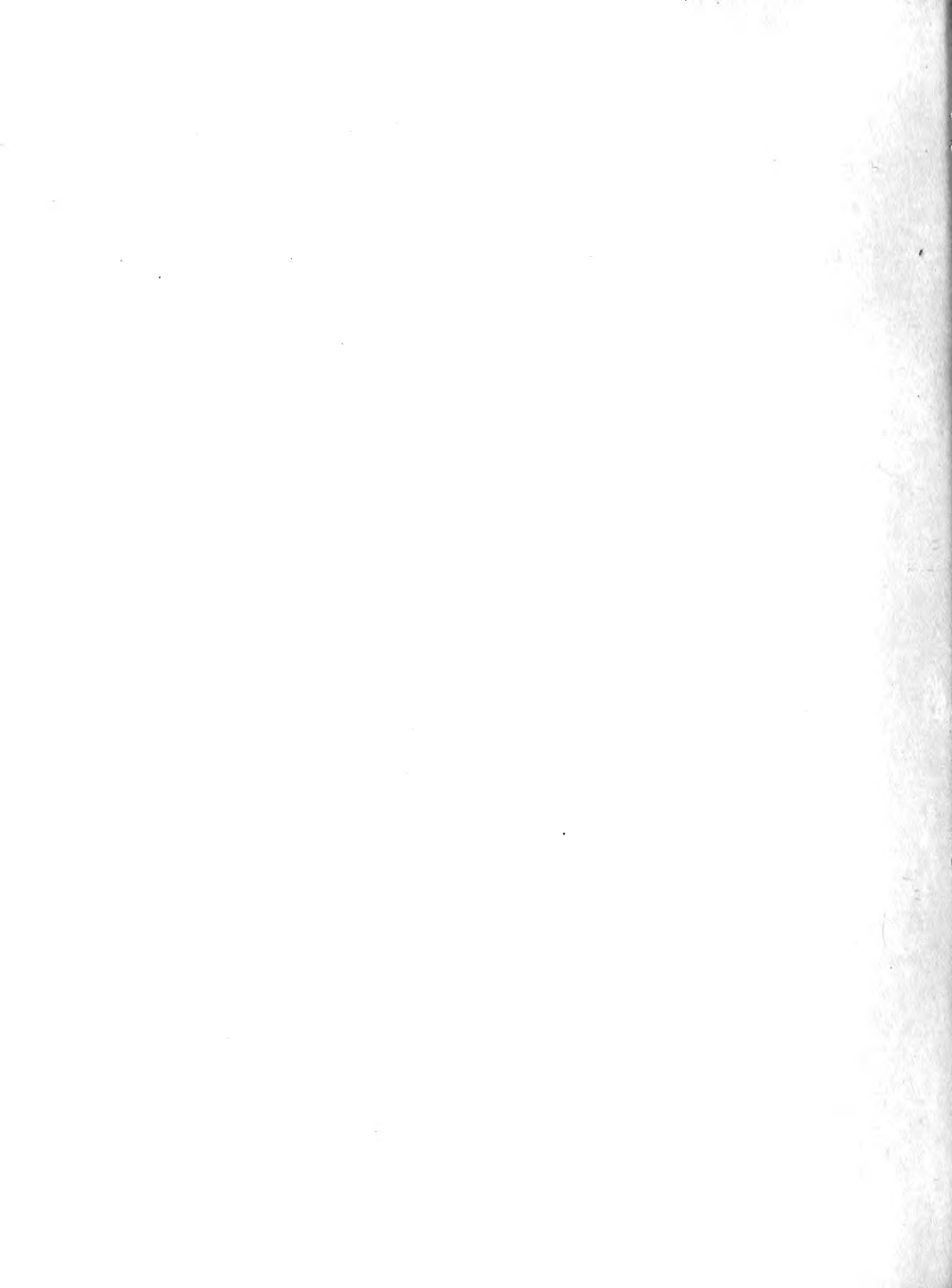
Progress Report #1



Published under the authority of the Secretary of the Navy

U. S. NAVY HYDROGRAPHIC OFFICE
WASHINGTON, D. C.
1952






FOREWORD

Since changes that occur in the thermal structure of the oceans have a far reaching effect on various naval operations, any practical technique that can be developed to predict these changes would have considerable operational utility.

This report represents the results of research concerning the effect of weather on the thermal structure of the ocean conducted by the Division of Oceanography up to 30 June 1952 under ONR Contract 260005. This project is being continued by the Hydrographic Office with periodic progress reports to be published at appropriate intervals.

It is requested that activities receiving this publication forward their comments to the Hydrographic Office.


KARL F. POEHLMANN
Captain, USN
Hydrographer

ABSTRACT

The purpose of this project is to investigate the meteorological factors that affect materially the thermal structure of the ocean and to develop techniques capable of predicting it. This report contains: (a) a description of the factors known to affect the thermal structure; (b) a summary of the known principles concerning each of these factors; (c) proposed prediction techniques based on these principles; (d) procedures and results of technique development so far undertaken by the project; and (e) proposals for future work by the project.

Two types of processes were studied: (a) those that are caused mainly by various meteorological variables; and (b) the process of vertical motion caused by internal waves. Those processes due to the horizontal field of motion were disregarded because of inadequate data.

Based on known or predicted meteorological variables, the processes of radiation, evaporation and molecular conduction, convection, and turbulent mixing are considered. The relationships giving the magnitude of the effect of these processes on the thermal structure are examined and typical values are presented under mean and extreme conditions. These relationships are fused into a proposed prediction technique.

A sample forecast illustrated by figures and graphs is made by considering the above processes and using the above mentioned techniques. Results are promising enough to warrant further consideration of the general approach. However, data presented indicate that an accurate and operationally useful



method of predicting the thermal structure cannot be obtained without consideration of the internal wave.

This problem is investigated by using two models, namely, the two-layer system and a model assuming the density to be a continuous function of depth.

Since the two-layer system assumes the wave to occur along the interface between fluids of different densities, the problem is simplified to the study of the oscillations of the thermocline with time. It appears that the main variations in the thermocline depths are: (a) seasonal variations; (b) lunar or monthly variations; (c) semidiurnal and diurnal tidal variations; (d) short period variations; and (e) random variations due to mixing. Data are presented to illustrate all these effects.

Because previous studies have shown (c) to be the largest single effect, it is studied empirically at some length. A formula is presented giving the amplitudes of these oscillations in one area as a function of the thicknesses of and density discontinuity between the layers by assuming a two-layer system on a rotating spherical earth. In the few cases in which the data were adequate for a forecast, the relationship predicted the amplitudes with a fair degree of accuracy.

When the continuous density model is considered, a more complicated picture of the internal oscillations results in which the amplitudes and phases vary continuously with depth. Methods are developed for predicting these internal oscillations and a sample prediction is presented. The observed and predicted



amplitudes show good agreement at the greater depths, but near the surface discrepancies occur. Possible reasons for these discrepancies are examined; it is proposed that deficiencies of the available data comprise the largest single factor.

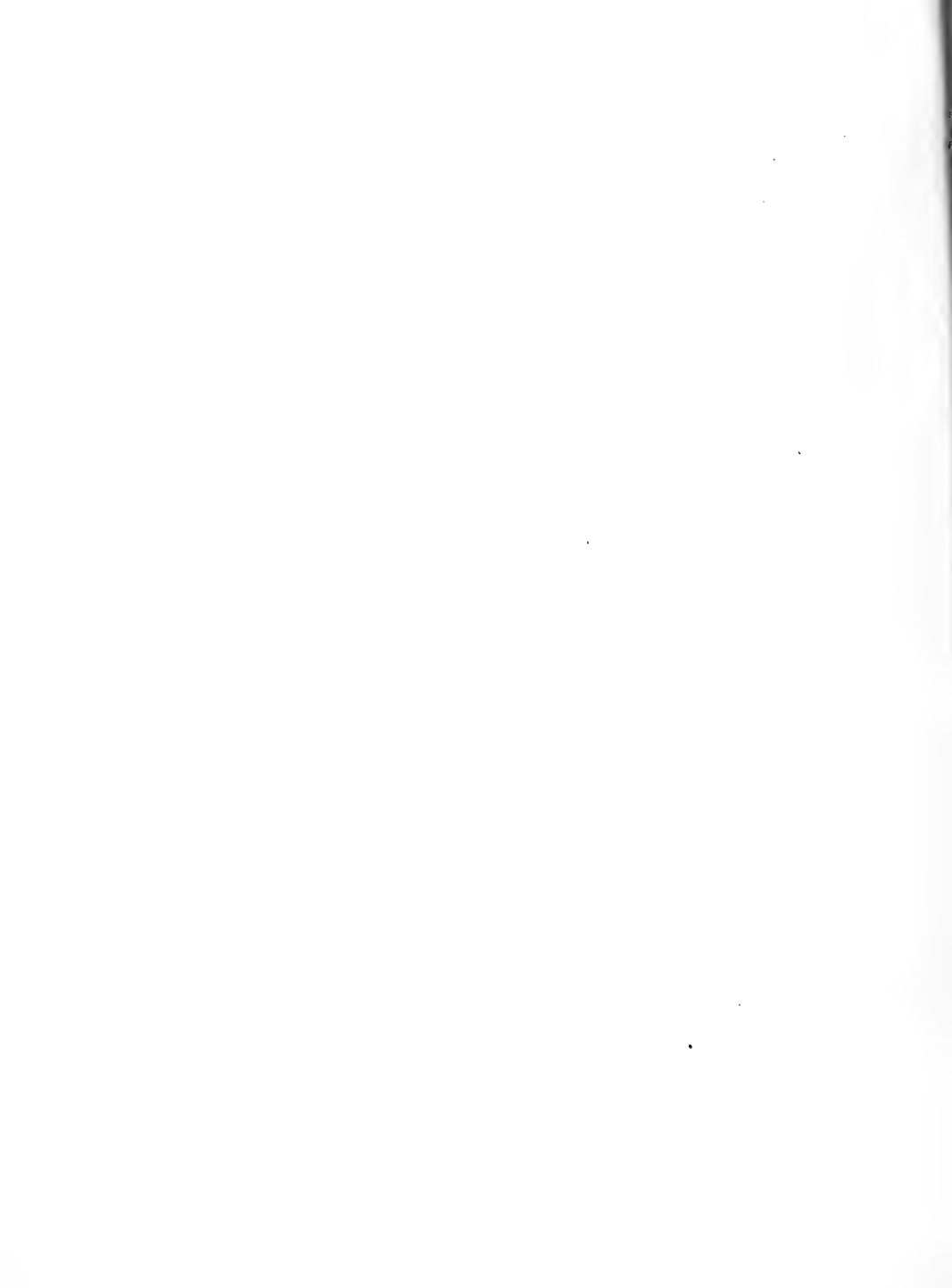
- - - - -

This report was prepared by J. J. Schule, Jr., with the assistance of L. S. Simpson and A. Shapiro.



TABLE OF CONTENTS

	Page
Foreword	iii
Abstract	v
List of Figures.	xi
List of Tablesxiii
I. Purpose.	1
II. Procedure.	2
A. Introduction	2
B. Direct investigation of meteorological parameters	4
1. Introduction	4
2. Thermodynamic Processes: Radiation.	4
3. Thermodynamic Processes: Exchange of heat between ocean and atmosphere	11
4. Mixing Processes: Convection.	12
5. Mixing Processes: Turbulent mixing.	16
6. Example of forecast.	19
C. Investigation of periodic variations due to internal waves.	32
1. Introduction	32
2. The two-layer system	33
3. The continuous density model	57
III. Data	68
IV. Recommendations for further work	72
Appendix A	74
Bibliography	79



LIST OF FIGURES

- Figure 1 Temperature changes over 3 days due to loss of heat from oceans to atmosphere.
- Figure 2 Change in thermal structure due to turbulent mixing.
- Figure 3 Pyrheliometer record, 1600-1800Z, 22 April 1951.
- Figure 4 BT trace, 0500Z, 20 April 1951.
- Figure 5 Transparency station, 23 April 1951.
- Figure 6 Energy spectrum of radiation from sun and sky at the surface.
- Figure 7 Change in temperature distribution due to radiation, 20-27 April 1951.
- Figure 8 Change in temperature distribution due to heat exchange with atmosphere and due to convection, 20-27 April, 1951.
- Figure 9 Change in temperature distribution due to mixing, 20-27 April 1951.
- Figure 10 BT trace, 2000Z, 27 April 1951.
- Figure 11 Generation of internal waves by an undersea ridge.
- Figure 12 Mean monthly mixed layer depths for weather ship COCA.
- Figure 13 Mean monthly mixed layer depths for weather ship DELTA.
- Figure 14 Mean monthly mixed layer depths for weather ship ECHO.
- Figure 15 Mean monthly mixed layer depths for Pacific weather ship NECTAR.
- Figure 16 Mean monthly mixed layer depths for Pacific weather ship GOLF.
- Figure 17 Mean monthly mixed layer depths for Pacific weather ship PAPA.

Date	Description	Amount
1/1/19	Balance forward	100.00
1/15/19	Deposited	50.00
2/1/19	Withdrawal	25.00
2/15/19	Deposited	75.00
3/1/19	Withdrawal	30.00
3/15/19	Deposited	60.00
4/1/19	Withdrawal	40.00
4/15/19	Deposited	80.00
5/1/19	Withdrawal	50.00
5/15/19	Deposited	90.00
6/1/19	Withdrawal	60.00
6/15/19	Deposited	100.00
7/1/19	Withdrawal	70.00
7/15/19	Deposited	110.00
8/1/19	Withdrawal	80.00
8/15/19	Deposited	120.00
9/1/19	Withdrawal	90.00
9/15/19	Deposited	130.00
10/1/19	Withdrawal	100.00
10/15/19	Deposited	140.00
11/1/19	Withdrawal	110.00
11/15/19	Deposited	150.00
12/1/19	Withdrawal	120.00
12/15/19	Deposited	160.00
1/1/20	Balance forward	170.00

LIST OF FIGURES

(Cont'd)

- Figure 18 Variation of the depth of the thermocline with time at weather ship DELTA, 1-22 August 1950.
- Figure 19 Daily variation of mean mixed layer depths for Pacific weather ship NECTAR, for the year 1948.
- Figure 20 Oscillations of the thermocline at weather ship DELTA, August 1950.
- Figure 21 Oscillations of the thermocline at Pacific weather ship 990, August 1944.
- Figure 22 Short period fluctuations of the thermocline at weather ship BRAVO, 2000-2200Z, 13 September 1945.
- Figure 23 Short period fluctuations of the thermocline at weather ship ALFA, 1500-1700Z, 22 September 1945.
- Figure 24 A Percentage distribution of mean daily thermocline depths.
- B Relationship between the amplitude of the tidal internal wave and the mean depth about which it oscillates. Pacific weather ship NECTAR and vicinity.
- Figure 25 A Percentage distribution of mean daily thermocline depths.
- B Relationship between the amplitude of the tidal internal wave and the mean depth about which it oscillates. Atlantic weather ship COCA and vicinity.
- Figure 26 Distance from trough to crest of the tidal internal wave as a function of the mean depth of the thermocline and various surface densities. Vicinity of Pacific weather ship NECTAR.

LIST OF TABLES

- Table I Typical daily temperature changes ($^{\circ}\text{F}$) due to the absorption of radiation at various latitudes and depth intervals.
- Table II Amount of heat ($\text{g. cal. cm.}^{-2} \text{ day.}^{-1}$) that is lost to the ocean due to exchange with the atmosphere for various wind speeds and sea-air temperature differences.
- Table III Mean daily values of various meteorological parameters for 20-27 April 1951.
- Table IV Computed and measured rates of total incoming and back radiation ($\text{g. cal. cm.}^{-2} \text{ min.}^{-1}$) for 20-27 April 1951.
- Table V Total heat (g. cal. cm.^{-2}) that is added to each layer of the water column because of absorption of radiation in the red and other spectral bands during the period 20-27 April 1951.
- Table VI Temperature changes in the various layers due to the absorption of radiation during the period 20-27 April 1951.
- Table VII Daily heat total (g. cal. cm.^{-2}) lost to the ocean, due to exchange with the atmosphere, for the period 20-27 April 1951.
- Table VIII Fourier coefficients as computed from anchor station of 4 Dec. 1950.
- Table IX Relative amplitudes, w , as computed from anchor station of 4 Dec. 1950.
- Table X Relative amplitudes, w , as computed from single density distribution on 9 Dec. 1950.
- Table XI Predicted Fourier coefficients for 9 Dec. 1950.
- Table XII Predicted and observed absolute amplitudes (meters) of the diurnal internal wave on 9 Dec. 1950.

I. Purpose

To investigate the effect of weather on the thermal structure of the ocean.

II. Procedure

A. Introduction

This project is aimed primarily at the eventual development of practical and operationally useful techniques for the prediction of the thermal structure of the ocean. Unfortunately, this is a complicated and difficult problem, for the thermal structure is affected by many processes, some of profound effect and all seeking to change its nature simultaneously. Separating these processes for study and estimating quantitatively their relative effects is therefore the first field of interest for this project. Added to the difficulties inherent in the problem itself is the fact that, in a science where controlled experimentation is impossible and data collection expensive, very little data adequate for an investigation of this type are available.

We may consider that the processes that affect the thermal structure may be divided into three classes: the thermodynamic, which involve a change in the heat content of the water column; the static, which involve temperature changes in the column due either to internal or external forces without change in the heat content; and the dynamic, which are the result of the three-dimensional field of motion. Under each we may list several processes:

1. Thermodynamic processes
 - a. Radiation - incident, reflected, and back radiation.
 - b. Exchange with atmosphere by molecular conduction.

- c. Exchange with atmosphere by evaporation.
- 2. Mixing processes
 - a. Convection
 - b. Turbulent mixing
- 3. Dynamic processes
 - a. Horizontal advection
 - b. Vertical advection due to internal waves

The parameters that affect the thermodynamic and mixing processes are mainly meteorological, such as air temperature and humidity, vapor pressure, wind, sea and swell, etc. It was therefore decided to attempt, by consideration of known principles, to evaluate the effects of these processes first, at the same time attempting to minimize the dynamic effects by testing these relationships with data collected in areas where large scale motions do not occur. If this attempt were successful, the dynamic effects then could be considered.

The following discussion should be considered more as an exposition of possible methods and techniques that might be utilized in attacking this problem than as a body of proven scientific results leading to a solution of the problem. Although several of the procedures tested yielded promising results, the few months that the project has been under way and the lack of available data have precluded the opportunity of testing a sufficient number of cases to demonstrate their validity conclusively:

B. Direct investigation of meteorological parameters

1. Introduction

We might divide the processes that depend on meteorological parameters and affect the thermal structure of the oceans into two classes: (1) the thermodynamic processes, which have to do with the actual addition or subtraction of heat from the ocean, and (2) the mixing processes, which cause changes in the thermal structure due to some internal or external force on the water column without changing the actual heat content of the column. The dynamic processes, which are those due to the three-dimensional distribution of motion in the oceans and the forces involved, have been neglected in this portion of the report.

2. Thermodynamic processes: Radiation

a. Incoming radiation

The most complete treatment of the energy exchange between the atmosphere and the ocean has been given by Jacobs (1942). Although this paper approached the problem from a climatological viewpoint, the relationships are of such a nature that, by knowing the values of the constants for a given area and being able to predict the values of the meteorological parameters involved, the total amount of heat gained or lost by the ocean during a given period may be determined. It is then necessary to translate this amount of heat into temperature changes; here the problem is complicated by the fact that we are interested not in the surface temperature change alone but in the change at every depth.

It is necessary to consider first the total amount of heat that reaches a unit area of the sea surface in a given time and is thus available to the water column for absorption at various depths. Mosby (1936) has shown that, with clear skies, the total incoming radiation may be accurately approximated by the simple linear equation

$$Q_0 = k\bar{\alpha} \quad (1)$$

Here Q_0 is the total incoming radiation expressed in g.cal. $\text{cm}^{-2} \text{min}^{-1}$. k may be considered as a parameter whose value varies with the water vapor in the atmosphere, but its variation is in such a narrow range that, for the purposes of this study, it may be considered as a constant and equal to 0.025. $\bar{\alpha}$ is the mean solar altitude, in degrees, during the period over which the heat is calculated.

This expression must be modified for cloudiness. This problem has been treated empirically by Angstrom (1922) and Kimball (1928). Their findings indicate that the values for the ration of overcast sky radiation to clear sky radiation vary between 0.22 and 0.30, the most likely mean value being 0.29. Applying this ratio, we have

$$Q_1 = .025\bar{\alpha} \left[0.29 + 0.71 \left(1 - \frac{\bar{C}}{100} \right) \right] \quad (2)$$

Here Q_t is the total amount of incoming solar energy reaching the sea surface in g. cal. $\text{cm}^{-2} \text{min}^{-1}$ and \bar{c} is the percentage of sky covered by clouds.

It is now necessary to apply a correction factor to equation (2) to account for the percentage of the incoming radiation that is reflected back to space. Schmidt (1950) has determined this percentage to vary from 3.3 at the Equator to 8.0 at the poles. Designating this percentage as r and applying it to equation (2), we have a final expression for the total amount of incoming radiation, namely,

$$Q_{ab} = .025 \bar{a} \left[0.29 + 0.71 \left(1 - \frac{\bar{c}}{100} \right) \right] (1-r) \quad (3)$$

Q_{ab} is still expressed in g. cal. $\text{cm}^{-2} \text{min}^{-1}$. If it is desired to calculate the total incoming radiation for some period of time, it is only necessary to multiply Q_{ab} by the period t expressed in minutes.

b. Back radiation

Not all of the heat energy defined in equation (3) is actually absorbed by the water mass. Some of this heat will be radiated back into space. Angstrom (1920) has defined a quantity, eff. Q_b , which depends on air temperature and humidity and gives the back radiation with a clear sky. These values are tabulated in Angstrom (1920) and are presented in nomogram form, slightly modified for a sea surface, in The Oceans (1942). This value also must be adjusted for the amount of cloudiness present and for internal reflection. When the most generally accepted

values for these corrections are applied, the following equation results:

$$Q_b = 0.94 [\text{eff } Q_b (1 - 0.0083 \bar{C})] \quad (4)$$

In this expression Q_b is the average back radiation in g. cal. $\text{cm}^{-2} \text{min}^{-1}$ and \bar{C} is the mean cloudiness in percent. Just as in the incoming radiation, for a finite period of time it is necessary to multiply Q_b by the period t expressed in minutes.

- c. Change in temperature with depth due to absorption of radiation

Subtracting Q_b from Q_{ab} will yield the amount of heat available for heating the oceans and for exchange with the atmosphere. To proceed with the investigation it was necessary to make two assumptions: (1) for sufficiently short period of time the processes of heating the water and of exchange of heat between ocean and atmosphere may be considered mutually exclusive processes and may be computed as such, and (2) each layer radiates in proportion to the radiation received.

Neglecting for the present the process of exchange with the atmosphere, therefore, we may write an expression for the temperature change at any depth, namely,

$$\Delta T_r(z) = \frac{f(z)}{C_p} (Q_{ab} - Q_b) \quad (5)$$

where

$\Delta T_r(z)$ = temperature change at depth z ,

C_p = specific heat of water at constant pressure (approximately 0.93)

There remains the problem of evaluating $f(z)$. This may be done in one of two ways. If the extinction coefficients for the area are known, we may employ the relationship

$$f(z) = e^{-kz} \quad (6)$$

Here k is defined as the extinction coefficient. For practical use it has become the convention in oceanography to consider k a constant over a meter's thickness; therefore, k is generally given per meter. For purposes of computation it is also more convenient to utilize equation (6) over succeeding intervals of one meter or more; if one meter is used, $z = 1$, if two meters are used, $z = 2$, etc.

Now, if we start at the surface with $(Q_{ab} - Q_b)$ and designate this quantity as Q_r , the amount of incoming heat left at the bottom of the first meter is

$$Q_{r_1} = Q_r e^{-k_1} \quad (7)$$

where k_1 is the extinction coefficient in the first meter. The amount of heat absorbed in the first meter is

$$\Delta Q_{r_1} = Q_r - Q_{r_1} = Q_r (1 - e^{-k_1}) \quad (8)$$

By continuing the process, the amount of heat remaining at the bottom of the second meter is obtained.

$$Q_{r_2} = Q_r e^{-k_1} e^{-k_2} = Q_r e^{-(k_1+k_2)} \quad (9)$$

where k_2 is the extinction coefficient between the first and second meters. The amount absorbed in the second meter is

$$\Delta Q_{r_2} = Q_r [e^{-k_1} - e^{-(k_1+k_2)}] \quad (10)$$

In general, the amount of heat absorbed in the n th layer is

$$\Delta Q_{r_n} = Q_r \left[e^{-\sum_{i=0}^{n-1} k_i} - e^{-\sum_{i=0}^n k_i} \right] \quad (11)$$

where $k_0=0$.

Now, dividing the values of ΔQ_r for the various layers by the thickness of the layers in centimeters and by c_p will yield the temperature change in that layer in $^{\circ}\text{C}$.

A simpler method of computing temperature changes at the different depths sometimes may be employed. When transparency stations are occupied at sea, the data may be collected in terms of the percentage of incoming radiation at the surface that is left at any given depth. If Q_r is known, therefore, the ΔQ_r for any layer may be computed directly from these data rather than from the extinction coefficients.

- d. Typical values of temperature changes at different depths due to the absorption of radiation

The above considerations have been used to compute the data presented in table I, which gives an indication of the magnitude of the temperature changes that might be expected at different depths and at various latitudes resulting from the absorption of radiation alone. These data were computed for a typical February and August day by using a reasonable mean altitude of the sun in each case. The percentage of cloudiness was assumed to be 50, and r was allowed to vary linearly with latitude within the limits described in section 2a above. The extinction coefficients were taken from a table of typical values for clear oceanic water presented on page 107 of The Oceans (1942)

Table I

Lat.	Total Heat Added (g.cal. cm. ⁻² day. ⁻¹)		Temperature Change °F							
			0-3 ft		15-13 ft		50-53 ft		100-103 ft	
	Feb	Aug	Feb	Aug	Feb	Aug	Feb	Aug	Feb	Aug
0°	353	349	2.29	2.26	.10	.10	.02	.02	.007	.007
30°N	152	402	0.93	2.60	.04	.11	.01	.02	.003	.008
70°N	-1.45	314	-	2.03	-	.09	-	.02	-	.006

Typical daily temperature changes (°F) due to absorption of radiation at various latitudes and depth intervals.

3. Thermodynamic processes: Exchange of heat between ocean and atmosphere

As has been discussed above, all the absorbed heat does not go into heating the oceans; some of the heat is lost from the water, because of exchange with the atmosphere. This exchange is composed of two processes, evaporation and molecular conduction. According to Jacobs (1942), both these effects may be incorporated into the following single relationship:

$$Q_e = 145.4 W t (e_w - e_a) \left[1 + 0.1 \left(\frac{T_w - T_a}{e_w - e_a} \right) \right] \quad (12)$$

where

Q_e = amount of heat gained or lost by the sea surface
in g. cal. cm^{-2}

W = wind velocity in knots,

t = time in days,

e_w = saturation vapor pressure over the water surface
(in. Hg.),

e_a = vapor pressure of the air (in. Hg.),

T_w = temperature of the water in $^{\circ}\text{F}$.,

T_a = temperature of the air in $^{\circ}\text{F}$.

An indication of the orders of magnitude of Q_e under typical conditions may be obtained from table II. These data were computed under the assumption that the air temperature was 60°F . and the relative humidity 75%. Values for Q_e are presented for various wind speeds and for various sea-air temperature differences by assuming that the process of exchange went on for one day only. It will be noted that with high

winds and large sea-air temperature differences, such as might be found north of a strong polar front, Q_e is extremely large and might easily be greater in magnitude than Q_p . When this occurs the net flux of heat per day is negative with respect to the ocean; therefore, to arrive at the new thermal structure it would be necessary to consider the process of convectational cooling to relatively great depths. If, however, the flux of heat is positive with respect to the oceans, the convection resulting from exchange with the atmosphere will take place within a relatively shallow layer because of marked surface stability. This is the reason why winter temperature traces are essentially isothermal to great depths whereas a shallow thermocline exists in summer. Superimposed upon this effect is the effect of turbulent mixing, which will further modify the thermal structure. The processes of convection and turbulent mixing will be discussed in the following paragraphs.

4. Mixing processes: Convection

So far we have developed the following constituents of a predicted thermal structure: (1) an amended temperature distribution, $T_p(z)$, which would result from a process of radiation alone (discussed in 2 above), and (2) an amount of heat, Q_e , which is to be lost to the water because of exchange with the atmosphere during the forecast period (discussed in 3 above).

Our problem now is to determine the modifications that will occur in $T_p(z)$ due to the loss of heat Q_e at the surface. When one considers this problem, it is necessary to consider

the effect of salinity on this new thermal structure. Practically, however, the only available data may consist of BT's with no accompanying salinity data. Therefore, it would be wise to consider possible methods for either eventuality.

a. If salinity data are not available in this case, we may write

$$Q_e = c_p \int_0^h [T_r(z) - T(h)] dz \quad (13)$$

where $T(h)$ is the temperature that exists from the surface to some depth h which must be chosen to satisfy the integral. Since the value of this integral, Q_e , is known, if $T_r(z)$ is known explicitly, then $T(h)$ may be easily calculated. However, since we do not always know the function explicitly, it is much more convenient to evaluate this integral graphically.

Since the units of Q_e are given in g. cal. cm^{-2} , the area, $[T_r(z) - T(h)] dz$ must have the units $^{\circ}\text{C cm}$. Since BT data is given in $^{\circ}\text{F}$. and feet, this area may be numerically evaluated by a simple conversion factor

$$Q_e = 16.95 c_p \int_0^h [T_r(z) - T(h)] dz \quad (14)$$

If it becomes convenient to use meters for depth instead of feet in plotting the curves, the conversion will then be

$$Q_e = 55.6 c_p \int_0^h [T_r(z) - T(h)] dz \quad (15)$$

An indication of how some of the typical values of Q_e

as given in table II may be applied to different types of temperature distributions is presented in figure 1. Here curve A might represent $T_p(z)$ (typical temperature change) for winter, and curve B for summer. To show the effect more clearly, Q_e was taken over a three-day period. In this figure the effect of the initial temperature distribution is noticeable. With a typical shallow summer thermocline, as is shown in curve B,

Table II

WIND SPEED (KNOTS)

$T_w - T_a$ (°F)	5	10	15
2	137	273	410
5	203	406	607
10	334	667	1000
15	457	913	1370

Amount of heat (g. cal. $\text{cm.}^2 \text{ day}^{-1}$) that is lost to the ocean due to exchange with the atmosphere for various wind speeds and sea-air temperature differences.

the change in temperature of the mixed layer will be much greater than with a deep thermocline for an equal loss of heat. In addition, it will be noticed that the sharper or more intense the discontinuity at the thermocline the less will be the change in the depth of the thermocline due to convective cooling.

b. If salinity data are available in addition to

temperature data, more accurate methods of predicting the thermal structure resulting from a given loss of heat, Q_e , at the surface are possible. Such methods already have been devised by Zubov (1938) and Defant (1949). Detailed descriptions and examples are given in the references and, since the methods were not employed in any of the examples used in this report, will not be repeated here. Essentially, the technique involves dividing a column of water into several small layers and, by successively mixing deeper and deeper layers, computing a new distribution of temperature, salinity, and density, as well as the amount of heat necessarily lost to the ocean to bring about this convection. In this way, it is possible to stop the process at the layer where this amount of heat loss is equal to the given amount Q_e .

5. Mixing processes: Turbulent mixing

We now have arrived at a predicted thermal structure which includes the effects of radiation, exchange of heat with the atmosphere, and convection. Let this temperature distribution be called $T_c(z)$. Depending on the amount of convection, this temperature distribution may or may not include a mixed layer, which may be called D_0 . The remaining problem is to determine whether there will be enough turbulence generated by the stress of wind or sea to cause the water to be mixed to a depth greater than D_0 .

No adequate practical techniques for attacking this problem exist in the literature. However, a possible approach to the problem was presented in an earlier progress report

of this project (Enc. Hydro ltr code 43-JH/mlb serial 3436). This approach is partly deductive, partly empirical in nature, and assumes that the depth to which mixing will occur is a function of three parameters:

a. The amount by which the predicted wind speed will exceed the critical wind speed V_c as demonstrated by Munk (1947).

b. The wave number, β , associated with the predicted sea state ($\beta = \frac{2\pi}{L}$).

c. The initial stability $\frac{1}{\rho} \frac{\partial \rho}{\partial z}$, designated by E.

Under these assumptions the following relationship was derived:

$$D = D_0 + \frac{K(V - V_c) t}{(1 + \frac{E}{A})(1 + \beta D)} + \frac{1}{4} \frac{\rho - \rho_0}{\rho + \rho_0} g t^2 \quad (16)$$

where

D = depth of thermocline due to mixing,

D_0 = original depth of thermocline,

A, K = constants of proportionality which must be determined by data,

ρ_0, ρ = density in mixed and unmixed layers, respectively,

t = time (units depend on units chosen for V and V_c).

Further work must be done to determine whether this relationship can be developed as a practical prediction tool. For this reason, prediction examples have been confined where possible to those cases where the mean value of V was less than the 13 knots given as the value of V_c by Munk.

Once the mixed layer due to turbulence D has been arrived

at, it is necessary to amend $T_c(z)$ to include this deeper thermocline. The temperature that the water will have through this mixed layer may be represented as

$$T_D = \frac{1}{D} \int_0^D T_c(z) dz \quad (17)$$

It is once again more convenient to evaluate this integral by graphical methods rather than determine the function $T_c(z)$ precisely. Figure 2 is an illustration of how this might be done. Since no heat is added or subtracted from the water column as was the case in Sec. 4 above, the area representing the heated portion should equal the area representing the cooling portion. A fair approximation may be made simply by counting squares. It should be mentioned that in this process the assumption must be made

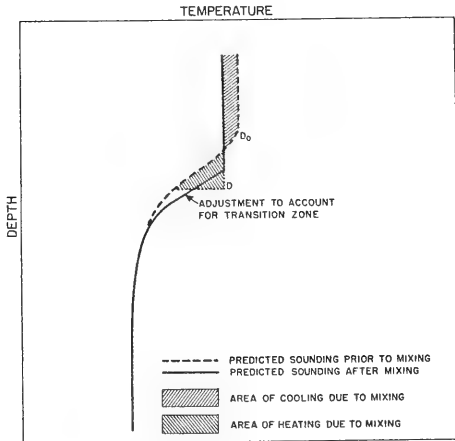


FIGURE 2. CHANGE IN THERMAL STRUCTURE DUE TO TURBULENT MIXING.

that the discontinuity between the new mixed layer D and the former sounding $T_c(z)$ is of zero order. Adjustment must be made for this, since it is known that the thermocline is not an ideal discontinuity but that a transition zone exists. This adjustment would have to be made in accordance with continuity of the past soundings and experience, which automatically brings in a factor of "art," as opposed to

"science," similar to that existing in modern weather forecasting. In figure 2 the final forecasted sounding is shown by the solid line.

6. Example of forecast

a. Introduction

The methods for estimating the effect of the meteorological parameters on the thermal structure, as outlined in Secs 2 to 5 above, were tested by attempting a prediction utilizing actual data. For this purpose there was available a collection of observations taken by the U. S. Navy Hydrographic Office on cruise AMOS VIII in April 1951. On this cruise, some of the latest instrumentation developed by the Oceanic Development Branch, Division of Oceanography, were employed. It was decided to utilize for the forecast that portion of the data gathered in the Sargasso Sea area, since here the data were more complete and the mean wind speeds were generally 12 knots or below, thus allowing the assumption that the turbulent effect was small. These data include: (a) hourly BT's; (b) hourly observations of meteorological variables; (c) hourly observations of sea and swell; (d) transparency stations using photocell equipment every few days; and (e) continuous pyrheliometer recording of incoming and outgoing radiation.

The type of radiation data available is illustrated in figure 3. It will be noted that these data were taken by three separate pyrheliometers, each recording directly the rate of radiation in $\text{g. cal. cm}^{-2} \text{ min}^{-1}$. Pyrheliometers 1 and 2 were mounted on either side of the ship to measure

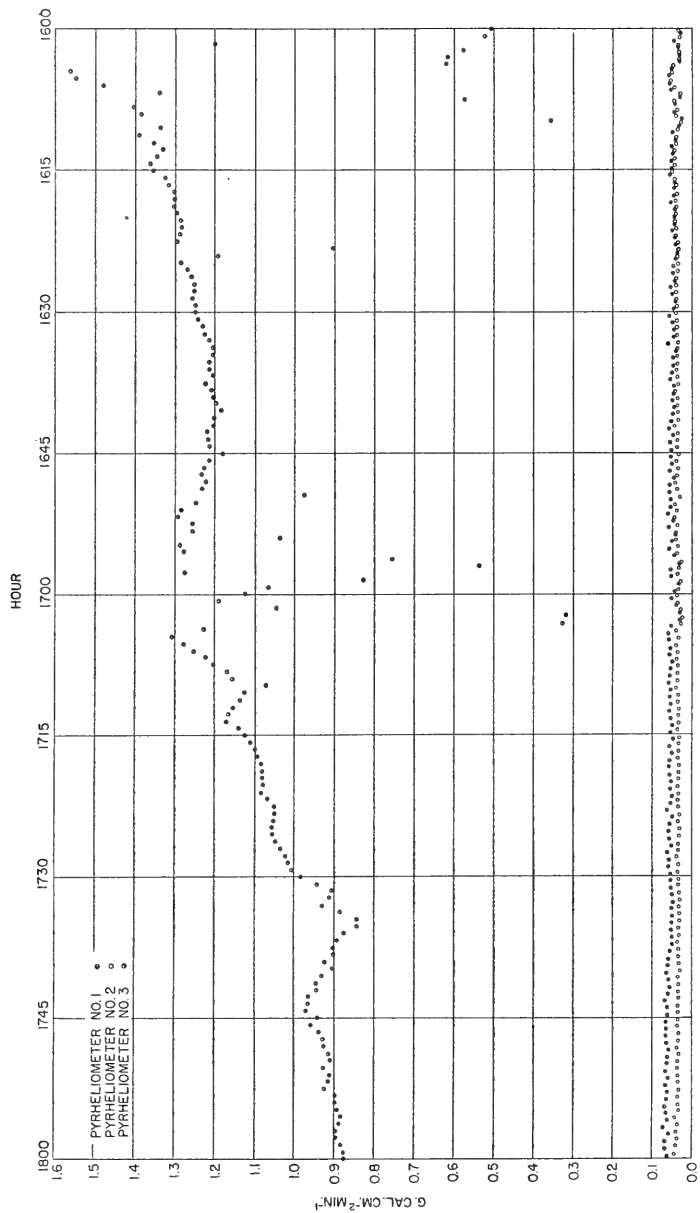


FIGURE 3. PYRHELIO METER RECORD, 1600-1800Z, 22 APRIL 1951.

back and reflected radiation from the sea surface; to arrive at the total effect the reading from the two instruments must be added. Pyrheliometer 3 measured the total incoming radiation from both sun and sky.

It was decided to attempt to forecast the changes in the characteristics of the thermal structure from the morning of 20 April to the evening of 27 April. A representative BT,

taken at 0500Z 20 April, was chosen as the initial temperature distribution. This BT trace is reproduced in figure 4 and plotted in meters for the sake of convenience.

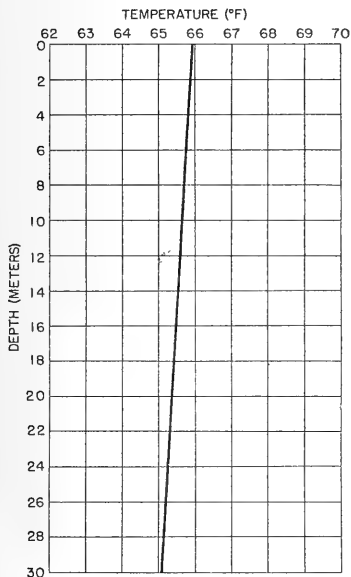


FIGURE 4. BT TRACE, 0500Z, 20 APRIL 1951.

each day, together with the mean daily altitude of the sun and the number of hours of sunlight. The values for the sun's altitude were extracted from tables in the air almanac for 1951 and H.O. Pub. No. 218, by assuming a mean daily hour angle of 45° during the daylight hours.

b. Procedure

- (1) Radiation (see Sec. 2 above)

Table III

Date	$\bar{\alpha}$ (deg)	No. of Hours of Sunshine	Sfc. Water T	Dry Bulb T	Wet Bulb T	e_w	e_a	\bar{C} (%)	Sea State	Wind Speed (knots)
20 Apr	43°30'	13	66.5	67.4	62.5	.649	.503	50	1	13
21 Apr	43°35'	13	66.4	66.2	60.7	.645	.468	60	2	3
22 Apr	43°54'	13	66.8	63.3	63.3	.656	.515	30	2	8
23 Apr	44°05'	13	65.8	64.5	58.8	.634	.440	50	3	13
24 Apr	44°15'	13	65.8	63.0	55.9	.634	.373	40	3	13
25 Apr	44°23'	13	66.2	64.5	55.9	.643	.353	40	2	8
26 Apr	44°40'	13	66.8	63.6	61.2	.656	.465	20	1	8
27 Apr	44°50'	13	66.9	67.8	61.5	.659	.472	40	2	8

Mean daily values of various meteorological parameters for 20-27 April 1951

The initial step was to calculate for each day the average value of Q_{ab} according to equation (3). These values for the total incoming radiation are given in the first column of table IV. In like manner, values for Q_b may be computed by using meteorological values given in table III and equation (4). These computed values for the back radiation appear in the second column of table IV. Both these sets of values are given in $\text{g. cal. cm}^{-2} \text{ min.}^{-1}$.

Table IV

Date	Computed ($\text{g. cal. cm}^{-2} \text{ min.}^{-1}$)		Observed ($\text{g. cal. cm}^{-2} \text{ min.}^{-1}$)	
	Q_{ab}	Q_b	Q_{ab}	Q_{ref}
20 Apr	.662	.096	.625	.100
21 Apr	.539	.081	.598	.090
22 Apr	.817	.125	.818	.110
23 Apr	.670	.096	.551	.100
24 Apr	.748	.113	.633	----*
25 Apr	.750	.117	.667	.095
26 Apr	.910	.140	.876	.120
27 Apr	.760	.112	.310	.100

*Inaccurate pyrhelimeter due to shock.
 Computed and measured rates of total incoming
 and back radiation ($\text{g. cal. cm}^{-2} \text{ min.}^{-1}$) for
 20-27 April 1951.

The first problem was to determine how closely the computed values for incoming radiation represented actual conditions during the forecast period. To do this pyr heliometer records were used. For each day during the daylight hours the average rate of incoming radiation was computed from the curve of pyr heliometer record number 3, by using finite differences at 15-minute intervals. These observed values are given in the third column of table IV. A similar process was carried out with curves of pyr heliometer record numbers 1 and 2. Adding the two gave the average daily rate of reflected radiation. These values for Q_{ref} are shown in the fourth column of table IV. The similarities between the computed and observed rates of incoming radiation, as shown in the first and third columns of table IV, are remarkable

The next step in the computation was to get the total incoming and back radiation for the eight-day period. Adding the values for Q_{ab} in the first column of table IV and multiplying by 13 hours or 780 minutes give a total incoming radiation of 4607 g. cal. cm^{-2} . Adding the values of Q_b in the second column of table IV and multiplying by 24 hours or 1440 minutes give the total of 1,267 g. cal. cm^{-2} . Subtracting Q_b from Q_{ab} gives a total of 3,339 g. cal. cm^{-2} absorbed by the water column during the period.

It is now necessary to convert this amount of absorbed heat to temperature changes with depth. A representative transparency station, occupied on 23 April, was chosen. These data were taken by the use of colored filters, thus giving a separate curve for each spectral band. Figure 5 presents the

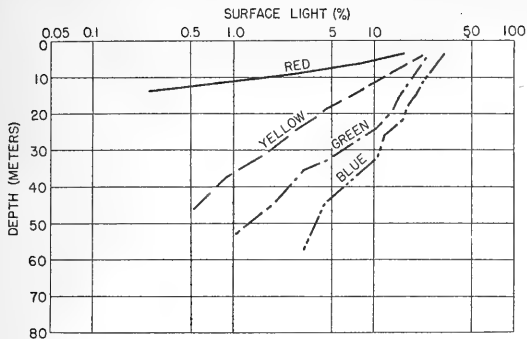


FIGURE 5. TRANSPARENCY STATION. 23 APRIL 1951.

data for the red, yellow, green, and blue portions of the spectra. For each of these bands the graph shows the percentage, on a logarithmic scale, of the incoming radiation that is left at any depth. The problem is to determine how much of the radiation is concentrated in each band. Figure 6 is an adaptation of a graph presented on page 105 of The Oceans (1942) showing the distribution of the energy spectrum at the surface of the radiation from sun and sky,

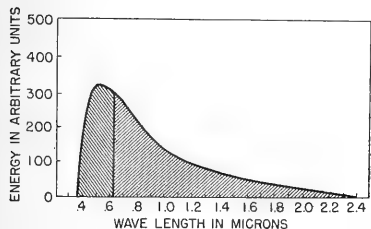


FIGURE 6. ENERGY SPECTRUM OF RADIATION FROM SUN AND SKY AT THE SURFACE.

plotted as a function of wave length. Taking 0.64 micron as the lower end of the red band and measuring the area under the curve, one arrives at a figure of 64.3% for the red and 35.7% for

the remaining bands. It was decided to use the curve for the green band as representative of the remaining 35.7%.

By starting with the total absorbed heat of 3,339 g. cal. cm^{-2} it now can be determined that 2,147 g. cal. cm^{-2} were absorbed from the red band and 1,192 g. cal. cm^{-2} were absorbed from all other bands. By using these figures in conjunction with the appropriate curve in figure 5, table V was constructed, showing the amounts absorbed from each band in each layer. The total number of g. cal. cm^{-2} absorbed in each layer for all bands

Table V

Layer (meters)	Red Band			Other Bands			Total Absorbed in Layer (g.cal. cm ⁻²)
	Entered Layer	Left Layer	Absorbed in Layer	Entered Layer	Left Layer	Absorbed in Layer	
0-4	2147	257	1890	1192	293	894	2784
4-6	258	172	86	298	274	24	110
6-8	172	36	86	274	250	24	110
8-10	36	39	47	250	226	24	71
10-15	-	-	-	226	203	23	23
15-20	-	-	-	203	155.0	48	48
20-30	-	-	-	155	72	83	83

Total heat (g. cal. cm⁻²) that is added to each layer of the water column because of absorption of radiation in the red and other spectral bands during the period 20-27 April 1951.

is shown in the extreme right hand column of table V.

To convert these totals of the amount of heat absorbed in each layer into temperatures, it is only necessary to divide by the number of centimeters in each layer and by Cp (.93). These temperatures will then be in °C; for use with BT data it is necessary to convert them to °F. Table VI gives the results of this computation with °C. in the left-hand column and °F. in the right-hand column.

Table VI

Layer (meters)	(°C)	(°F)
0-4	7.48	13.4
4-6	.590	1.06
6-8	.590	1.06
8-10	.380	.684
10-15	.050	.090
15-20	.100	.180
20-30	.090	.162

Temperature changes in the various layers due to the absorption of radiation during the period 20-27 April 1951

The final step is to apply the temperature changes given in table VI to the original trace as shown in figure 4. The

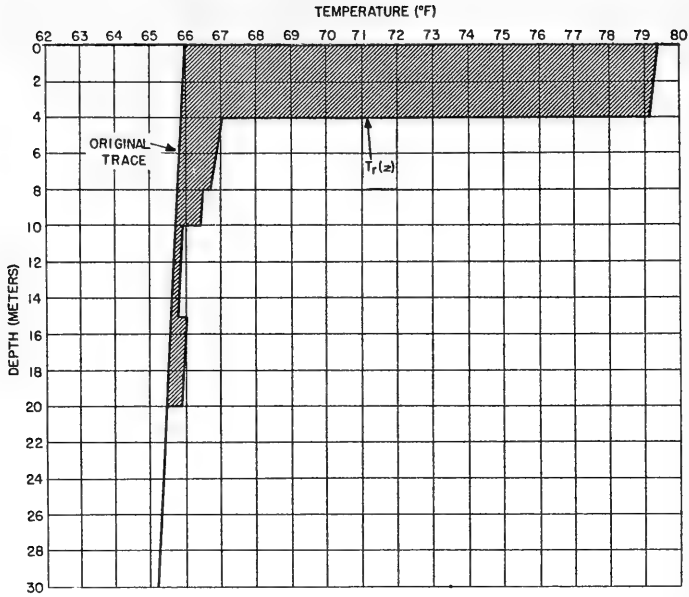


FIGURE 7. CHANGE IN TEMPERATURE DISTRIBUTION DUE TO RADIATION, 20-27 APRIL 1951.

resulting temperature distribution is $T_r(z)$, and is shown in figure 7.

(2) Heat exchange with atmosphere (see Sec. 3 above)

It is now necessary to compute the amount of heat gained or lost by the ocean from exchange with the atmosphere. This may be done easily for each day of the forecast period by the use of equation (12) and the meteorological data presented in table III. The results of Q_e for each day are presented in table VII. Addition of these daily values of Q_e gives a total of 2,322 g. cal. cm^{-2} , which is the total heat lost to the ocean by exchange with the atmosphere.

Table VII

Date	Q_e (g.cal.cm ⁻² day ⁻¹)
20 Apr	253.97
21 Apr	219.83
22 Apr	140.75
23 Apr	391.27
24 Apr	546.28
25 Apr	357.10
26 Apr	201.24
27 Apr	207.06

Daily heat totals (g. cal. cm⁻²) lost to the ocean, due to exchange with the atmosphere, for the period 20-27 April 1951.

(3) Convection (see Sec. 4 above)

$T_r(z)$ now must be adjusted to take care of the total heat, Q_e , lost to the ocean as computed above. Since figure 7 is plotted in °F. and meters, it is necessary to employ equation (15) in this computation. Substituting for Q_e the total given above and solving for the integral, we obtain

$$\frac{2322}{55.6 \times 93} = \int_0^h [T_r(z) - T(h)] dz = 44.92 \text{ °F meters} \quad (18)$$

Here 44.92 is the number of squares, bounded by one meter and one °F., which must be subtracted graphically from $T_r(z)$ to arrive at the predicted temperature distribution. This is done in figure 8, and the resulting distribution is $T_c(z)$.

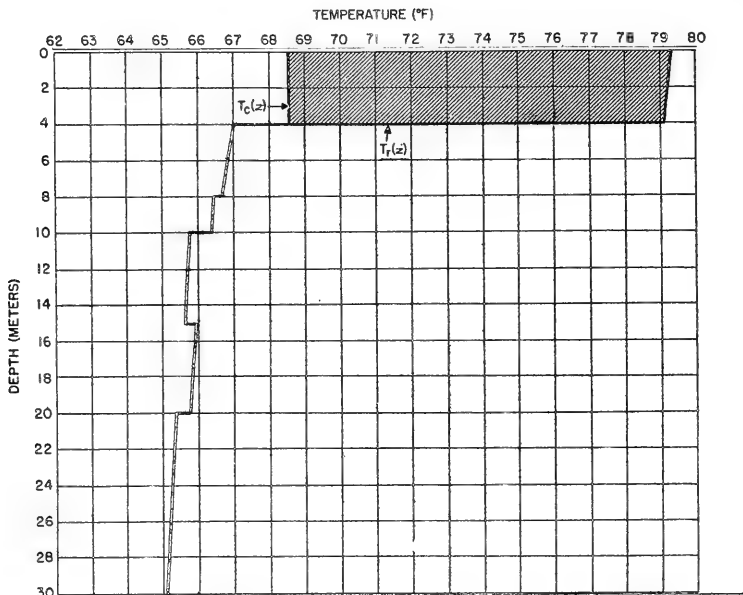


FIGURE 8. CHANGE IN TEMPERATURE DISTRIBUTION DUE TO HEAT EXCHANGE WITH ATMOSPHERE AND DUE TO CONVECTION. 20-27 APRIL 1951

(4) Turbulent mixing (see Sec. 5 above)

The character of $T_c(z)$ was so unusual that it was considered probable from past experience that the wind and sea would be of enough force to mix the shallow layer in which two abrupt discontinuities are shown. Some of this abruptness undoubtedly is due to the discontinuous manner in which the temperature changes due to radiation must be plotted. Therefore, $T_c(z)$ was adjusted by graphic means according to the

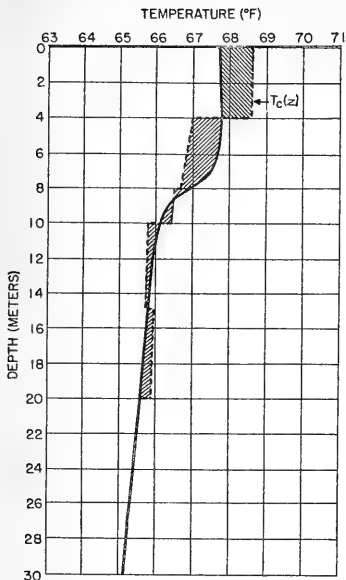


FIGURE 9. CHANGE IN TEMPERATURE DISTRIBUTION DUE TO MIXING, 20-27 APRIL 1951.

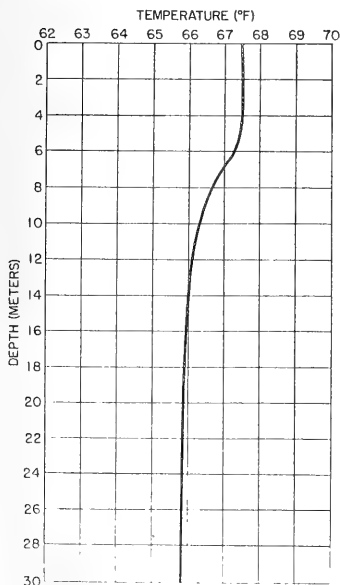


FIGURE 10. BT TRACE, 2000Z, 27 APRIL 1951

principles of equation (17) and figure 2. Figure 9 shows the results of this adjustment; the final forecast sounding for the evening of 27 April is shown by the solid line. Figure 10 shows a BT observation which may be used as a verification of this forecast, having been taken at 2000Z on 27 April. Except for a slight discrepancy in surface temperature, the agreement between the predicted and observed temperature distribution must be considered good.

If the depth of the thermocline as predicted above would remain constant for a reasonable period of time, it could be concluded that a possible method of predicting the thermal structure had been developed. However, another factor remains which requires investigation. It is noted that the thermocline oscillates in a periodic manner which in no way can be attributed to the effect of meteorological variables. It was considered that this problem must be considered before adequate means of predicting the thermal

structure could be developed. These oscillations, the so-called internal wave, are the subject of the following section of the report.

C. Investigation of periodic variations due to internal waves

1. Introduction

The problem of periodic oscillations of the water masses in the oceans has been treated by various authors in the past, and more and more attention has been given this phenomenon in recent years with the increasing realization of the important role these waves play in the determination of the thermal structure. The problem of isolating these waves from other processes operating in the ocean is not a simple one; one of the facts that has become evident to all investigators of internal waves is that these waves complicate the actual motion greatly and cause extremely varied and intricate distributions of currents and vertical motions.

In general the problem has been approached in two ways. The first is the simpler linear theory first treated by Stokes (Lamb, 1932) in which it is assumed that the wave occurs along the discontinuity surface between two layers, each homogeneous and each of different density. The more complex problem of progressive internal waves in a heterogeneous medium in which density is a continuous function of depth has been attacked with considerable success by Fjeldstad (1933) and others. In oceanography both models have their applications, and therefore both have been considered in this investigation.

Before proceeding with a discussion of how the two separate models were approached, it might be well to mention that the general conclusion reached by most investigators is that the greatest single factor in determining the nature of the thermal structure at any one time is the internal wave of tidal period. Consequently most of the investigations have centered around waves of semidiurnal and diurnal periods.

2. The two-layer system

This problem resolves itself mainly into a consideration of the depth and the amplitudes of the oscillations of the thermocline, because of the fact that the maximum amplitude of the wave occurs at the interface between two layers of different densities. It also can be shown, from the boundary conditions and the fact that density is constant through each layer, that the amplitude must decrease linearly from the interface and approach zero at both the free surface and the bottom.

Although the problem of the internal wave was first attacked by Stokes (Lamb, 1932), who derived a good many of the relationships, the subject did not excite much practical interest until the work of Ekman (1904). Ekman used the concept of the internal wave to explain the peculiar phenomenon of "dead water" experienced by slow moving sailing vessels and steamships of that period. He showed that when "dead water" was experienced, there existed a layer of light, fresh water overlying a heavier, more saline water below. The energy which the ship usually used to overcome the resistance of the water itself went instead to the generation and maintenance of

an internal wave along this boundary, with a resultant hindrance of the forward motion of the ship.

Vertical displacements of water masses may be easily observed by repeating, at short time intervals, oceanographic observations at one place. The first investigation of this type was made by Helland-Hansen and Nansen (1909) on the Michael Sars expedition. During the cruise repeated serial observations were made by two ships and a harmonic analysis was made of the data.

If such observations are repeated for a long enough time, it is possible to find by harmonic analysis the period of the waves. Although short periodic internal waves such as were described by Ekman are known to exist and are actually observed, the Michael Sars data yielded the information that the predominant periods of the oscillations were of semidiurnal and diurnal nature.

This conclusion has been borne out by the work of other authors. One of the most complete analyses of such data was made by Seiwel (1939, 1942). The results of this investigation showed that, after the oscillations of 12- and 24-hour periods were eliminated, the residue exhibited a normal or random distribution. Seiwel also demonstrated that, not only did the diurnal and semidiurnal waves predominate in period, but they also made the greatest contribution to the amplitude of the waves.

Although these investigations have demonstrated that the vertical oscillations in the oceans are dominated by waves of

12- and 24-hour periods, the difficulty has been to show that these waves have their origin in the tidal forces. Defant (1932) and others have shown that the tidal force is not sufficient to account for the observed amplitudes of these waves directly. He suggests that these oscillations may not be due to true internal wave motion at all, but rather are the result of periodic variations with time of the horizontal tidal currents, which cause periodic variations of the inclinations of an existing surface of discontinuity.

Another objection to the thesis that these waves are of a tidal nature has been the fact that when the velocity of propagation of these waves was computed, it was found to be much less than the velocity of the surface progressive tidal wave. Therefore, it was concluded that no resonance between the tidal forces and the responding medium could occur. Since the vertical component of the tidal force is not sufficient to cause the wave directly, and since no resonance could take place, it seemed to some highly unlikely that these waves had their origin in the tidal forces.

This problem has been attacked by Haurwitz (1950), who attempted to show that resonance could occur if one considered the effect of the earth's rotation. When this factor is considered, one arrives at free wave periods which are much closer in magnitude to the semidiurnal and diurnal periods. Haurwitz also suggests that, if the procedure were altered to include consideration of a rotating spherical earth rather than a rotating disc, much closer agreement might be obtained. This is still to be shown; the present investigators have made an attempt, but

the results in their unsimplified form are too unwieldy to be of much practical value. (See appendix A.)

Another interesting treatment has been presented by Zeilon (1911). In this paper he stresses the importance of the bottom configuration in generating and maintaining oscillations in the ocean. He discusses a model in which a uniform steady current encounters an elevation in the bottom topography. He shows that under these conditions a wave will be generated downstream from the elevation and, from continuity considerations, will also extend

upstream. The greatest internal wave amplitude will be in the vicinity of the elevation. Figure 11, taken from Zeilon's work, illustrates this effect.

Zeilon's work is mentioned to suggest that the bottom contours play some part in the formation of internal waves. It is therefore advisable in any study of this phenomenon either to take this effect into account or to eliminate it.

It was decided in this study to utilize data taken in one locality in order to eliminate bottom topography effects.

In discussing the two-layer system, mention should be made of a

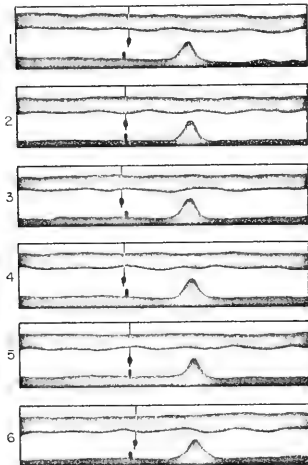


FIGURE 11 GENERATION OF INTERNAL WAVES BY AN UNDERSEA RIDGE.

Diagram of series of six photographs taken at intervals of about one-half second, showing the generation of waves in the boundary above the ridge and their propagation on both sides of it. To the left of the ridge is visible a small pendulum indicator, moving with the water and showing the direction and intensity of the current.

new approach formulated by Davies(1951). This paper has not as yet been studied thoroughly, but in the future the practical applications of this work to the present problem will be evaluated.

Since the basic assumptions made in the simplified two-layer model predicate the wave to be traveling along the interface, a study of the internal wave using these principles must mainly be a study of the oscillations of the thermocline. One may begin by defining the processes which, at any given time or for any period of time, will govern the depth of the mixed layer. These are:

a. Seasonal variations - Probably more is known about this parameter than any other because it is strongly reflected in the mean monthly values of the thermocline, which mean values have been published.

Illustrations of this effect, taken from these publications, are given in figures 12, 13, and 14. Since most of the time-series BT data are

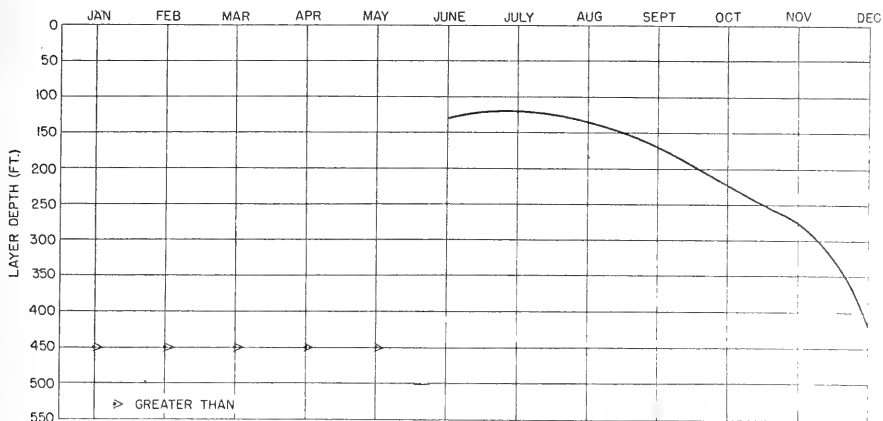


FIGURE 12. MEAN MONTHLY MIXED LAYER DEPTHS FOR WEATHER SHIP COCA, 52.7°N, 35.7°W.

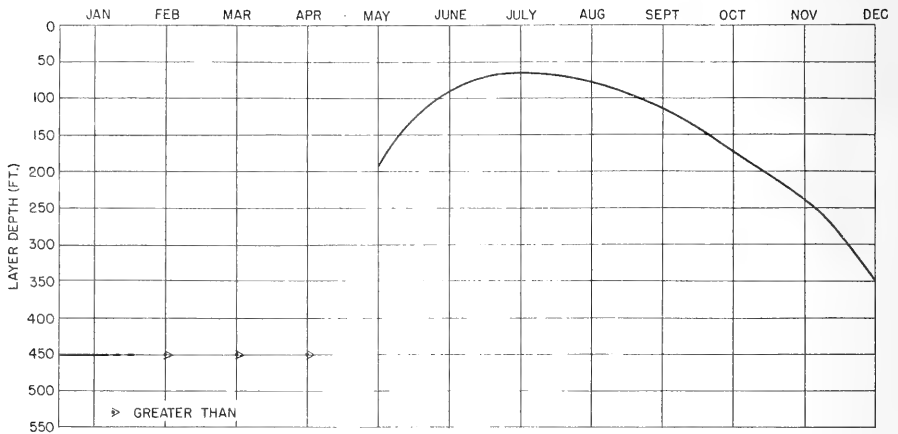


FIGURE 13. MEAN MONTHLY MIXED LAYER DEPTHS FOR WEATHER SHIP DELTA, 44°N, 41°W

collected from weather ships, these graphs show the monthly march of mixed layer depth at Atlantic weather ship stations COCOA, DELTA, and ECHO. The features of these graphs are familiar. As a result of excess absorbed insolation over emitted radiation, the thermocline forms in late spring and early summer and is driven progressively deeper by continued mixing during the late summer and autumn, until it becomes indistin-

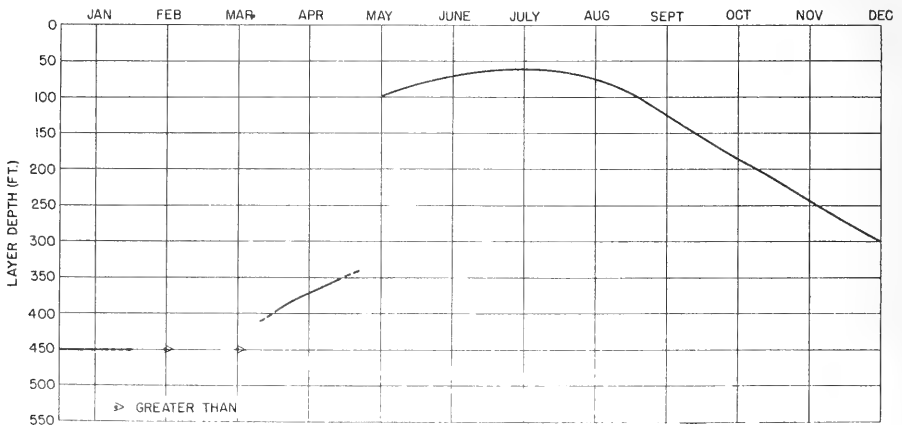


FIGURE 14. MEAN MONTHLY MIXED LAYER DEPTHS FOR WEATHER SHIP ECHO, 35°N, 48°W

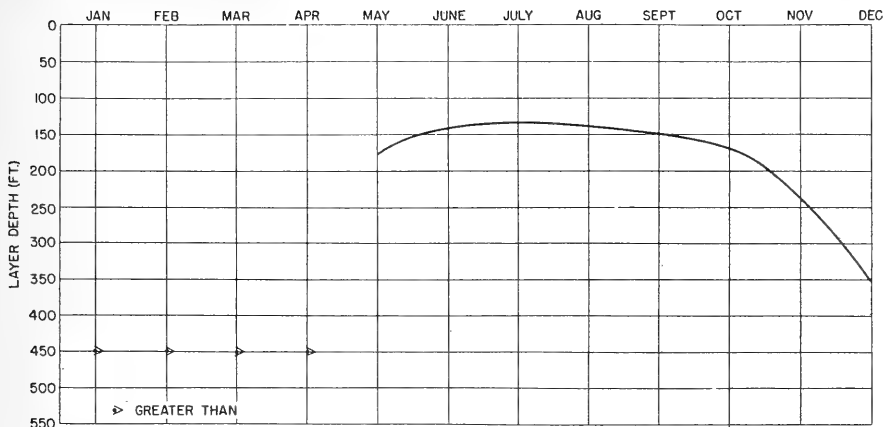


FIGURE 15. MEAN MONTHLY MIXED LAYER DEPTHS FOR PACIFIC WEATHER SHIP NECTAR, 30°N., 140°W.

guishable below 450 feet. Minor variations with latitude are noted. Figures 15, 16, and 17 give the same type of presentation for three Pacific weather ship stations, computed from the BT data on file at the Hydrographic Office. In these Pacific data it will be noted that, in the early summer, more than one value for the mean depth of the thermocline is shown (figure 16). This is the transition period when the old, deep winter thermo-

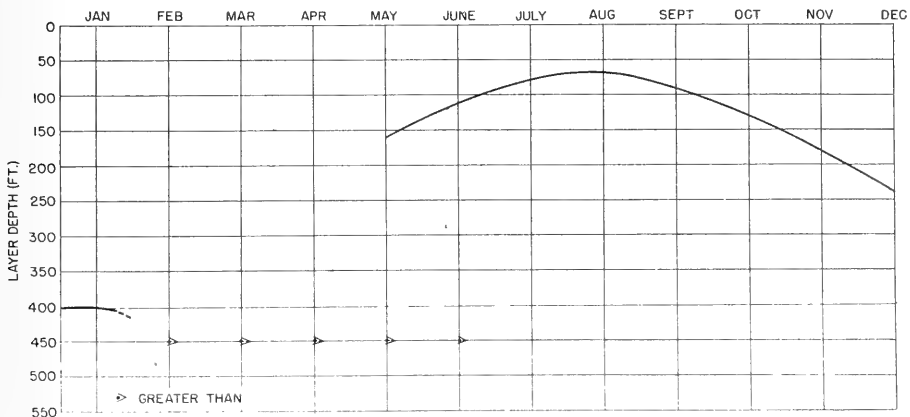


FIGURE 16. MEAN MONTHLY MIXED LAYER DEPTHS FOR PACIFIC WEATHER SHIP GOLF, 38°N., 158°W.

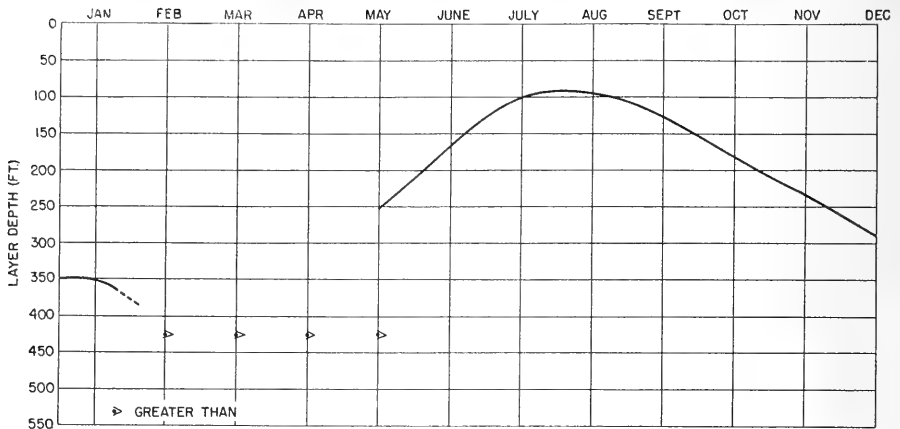


FIGURE 17. MEAN MONTHLY MIXED LAYER DEPTHS FOR PACIFIC WEATHER SHIP PAPA, 50°N, 145°W.

cline is sometimes still in evidence and at the same time the new, shallow thermocline is forming. A mean between the two would not only be unrepresentative of actual conditions, but would give the impression that there is continuity to the curve of mean monthly layer depths. Naturally this is not the case; one thermocline is distinctly different from the other.

b. Monthly or lunar variations - In working with time-series BT data, it was noted that long period fluctuations seemed to exist with periods suggestive of monthly oscillations, and superimposed on the seasonal variations, as illustrated in figure 18. It was considered that, if such fluctuations actually exist, they cannot be attributed to turbulent mixing caused by winds or sea. Although turbulence will cause an increase in the depth of the thermocline, there is no reason to expect the thermocline to rise gradually when the wind or sea subsides. Instead, the original thermocline should remain deep after the turbulence ceases, and with renewed mixing by wind and sea, a new mixed

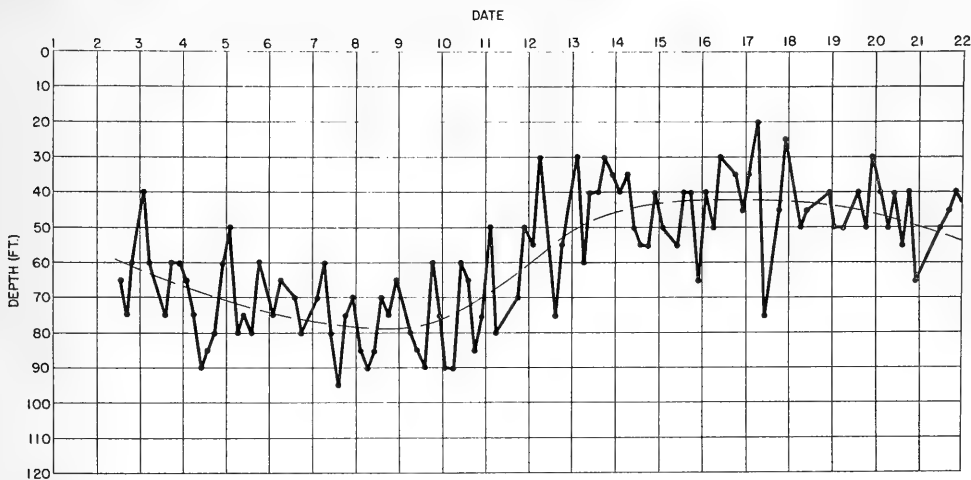


FIGURE 18. VARIATION OF THE DEPTH OF THE THERMOCLINE WITH TIME AT WEATHER SHIP DELTA, 44°N, 41°W, 1-22 AUGUST 1950.

layer should form. Since the wave motion observed does not conform to this description, some other factor must be at work.

In an attempt to discover if a 29-day lunar variation in the thermocline exists, the most complete set of daily BT observations available for one year was plotted. These data were for the year 1948 at the Pacific weather ship NECTAR. An attempt was made to eliminate the shorter period variations by plotting the mean value for each day rather than each single observation. This method was not successful because too many days had only one or two observations instead of the expected six; consequently, it was impossible to tell in which phase of the daily oscillation this single observation was taken. Since short period variations still appeared on the curve, a regression curve was computed to eliminate them, as shown in figure 19. In this graph the seasonal variation already discussed is apparent and, in addition, a suggestion of ridges and troughs appears in the

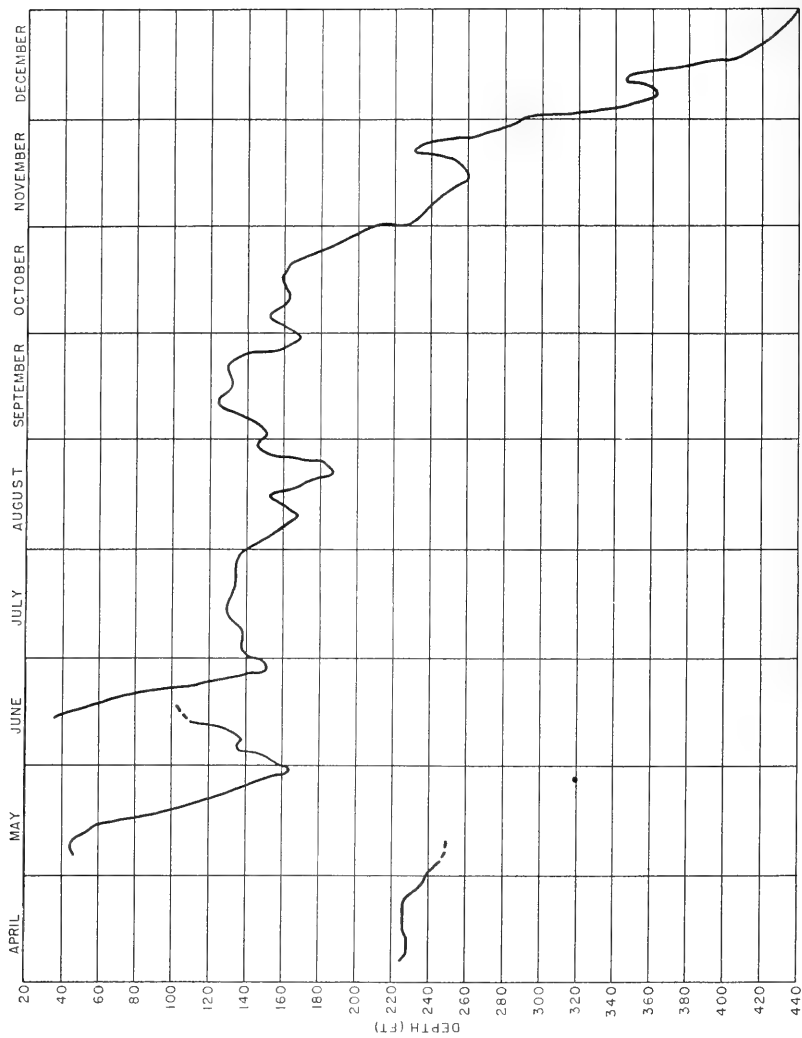


FIGURE 19. DAILY VARIATIONS OF MEAN MIXED LAYER DEPTHS FOR PACIFIC WEATHER SHIP NECTAR, 30°N, 140°W, FOR THE YEAR 1948.

curve with periods of approximately one month. Fourier analysis was applied to these data in an attempt to discern a true 29-day cycle; the results were negative. This fact is not surprising, since so many other parameters affect the depth of the mixed layer that any monthly variation must be treated not as a total cause in itself, but rather as a partial cause together with other causes. This technique will be discussed later.

c. Semidiurnal and diurnal tidal variations - It has already been mentioned that previous investigators have concluded that the greatest short period variations in the depth of the thermocline have their origins in an internal wave of tidal character. For this reason the main emphasis has been placed on attempting to discover techniques which would predict this effect.

The simplest technique one can use in this case is a purely statistical one, such as is used in predicting the tides themselves. It was noticed that some of the time-series traces of the thermocline variations at ship stations in the Eastern Pacific bore a marked resemblance to the tidal curves at stations on the West Coast of the United States. Some of the best data, therefore, were given to the U. S. Coast and Geodetic Survey with a view to having the data analyzed for the presence of semidiurnal and diurnal constituents and eventual prediction of the depth of the thermocline by means of constants. It was fully realized that the depth and intensity of the thermocline have an effect on both the amplitude and phase of the wave, but it was hoped that the results would be useful for a particular place by using a different set of constants for each location.

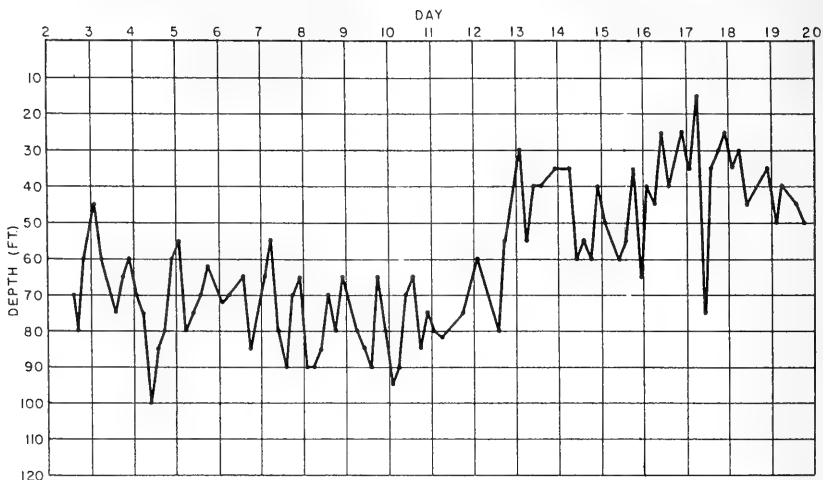


FIGURE 20. OSCILLATIONS OF THE THERMOCLINE AT WEATHER SHIP DELTA, 44°N, 41°W., AUGUST 1950.

The analysis of the Coast and Geodetic Survey, however, proved negative. It was their opinion that there were deficiencies in the data, since, with the number of daily observations varying from only one to six, one cannot be sure that the peaks and troughs of the waves are clearly defined. There is no doubt also that the effect of the depth and the vertical density gradient upon the change in phase and amplitude of the wave with depth was also a major contributing factor to the failure of such an attempt. Illustrations of the type of data which were analyzed in this manner are given in figures 20 and 21. The irregularities in the amplitudes would lead one to believe that the point of the Coast and Geodetic Survey is well taken. For a complete statistical analysis, observations should be taken at much more frequent intervals, in order that the curve more closely approximate a continuous trace and all the ridges and troughs be delineated.

d. Short period internal waves - In addition to the above

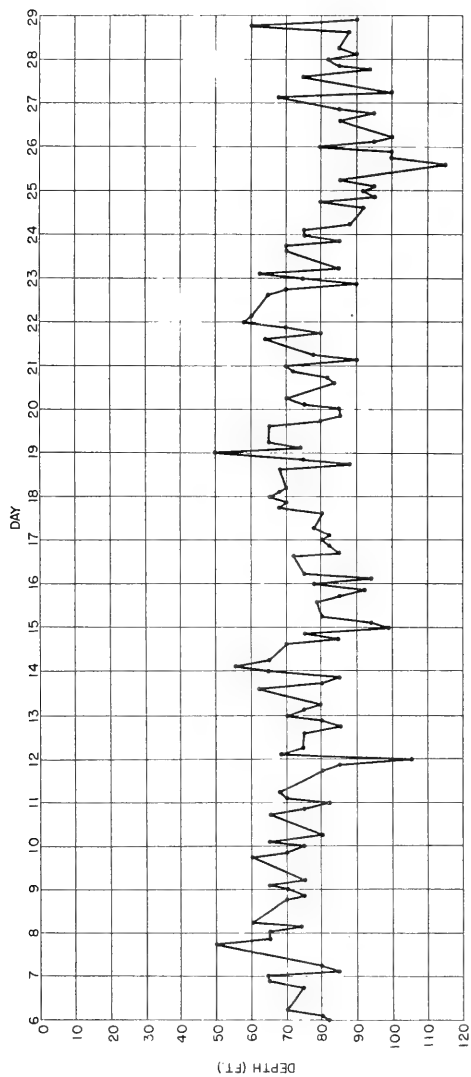


FIGURE 21. OSCILLATIONS OF THE THERMOCLINE AT PACIFIC WEATHER SHIP 990, 40°N, 150°W., AUGUST 1944.

mentioned periodic motion, there are known to exist in the oceans internal waves of periods of the order of magnitude of a few minutes. The most complete treatment of these short period internal waves has been given by Ufford (1947 a, b, c). These papers derive relationships giving the amplitude, period, and wave length of these waves for several special cases of multilayered systems. Ufford's work seems to give promise of being of practical value in the study of these waves, although as yet the present project has not been extended beyond consideration of the semidiurnal and diurnal periods, Data have been collected, however, which illustrate this effect, and examples are given in figures 22 and 23. It will be noted in figure 22 that superimposed on what is possibly the major semidiurnal tidal variation are many small oscillations of a period of a few minutes.

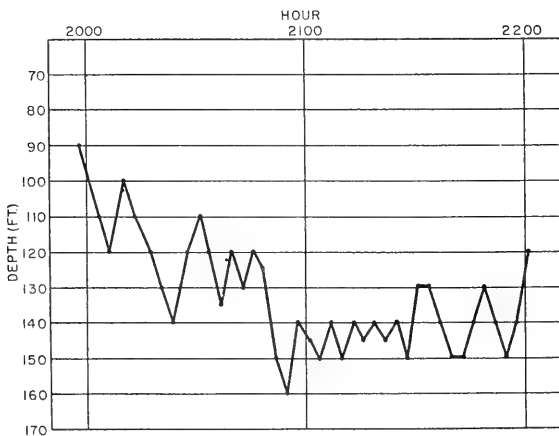


FIGURE 22. SHORT PERIOD FLUCTUATIONS OF THE THERMOCLINE AT WEATHER SHIP BRAVO, 56°N, 51°W, 2000-2200Z, 13 SEPTEMBER 1945.

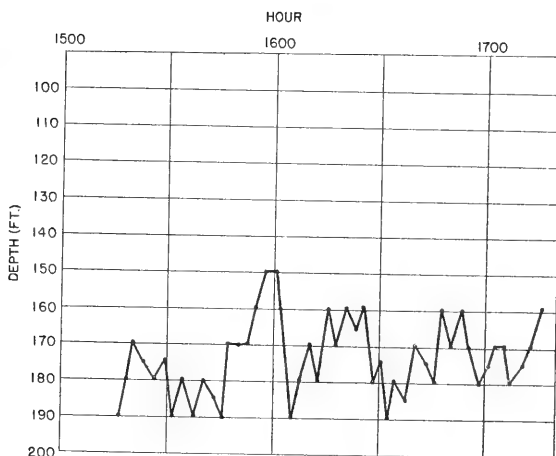


FIGURE 23. SHORT PERIOD FLUCTUATIONS OF THE THERMOCLINE AT WEATHER SHIP ALFA, 61°N, 33°W, 1500-1700Z, 22 SEPTEMBER 1945.

There is little doubt that short period oscillations as described above is one of the main factors that cause discrepancies between theoretically computed and actually observed sonar conditions. However, the limitations of the available data have made it impossible to approach this problem in conjunction with the longer period waves. It is hoped that in the future arrangements can be made for such data to be collected and the problem investigated.

e. Random variations due to mixing - Since the mechanisms that cause mixing in the ocean are mainly meteorological in nature, this problem has been discussed in the earlier portion of this report. It was concluded that there were two main processes that affect the depth of the thermocline: convectational mixing due to instability, and turbulent mixing due to wind and sea. When the random effects of these two processes are superim-

posed on the periodic variations discussed above, a highly irregular pattern results. When these data are subjected to an empirical treatment, there are two difficulties which must be overcome. One is the problem of determining the proper lag factor to employ, because the thermal structure does not reach equilibrium with the sea and wind instantaneously. The other is the fact previously mentioned, namely, that while turbulent mixing causes the thermocline to get deeper, ceasing of the turbulence does not necessarily cause the thermocline to become shallow.

1. Empirical investigation of thermocline depth - With all the effects described above existing at the same time and in view of the limited data available, it would be difficult to correlate any one of these single parameters with the variation in the thermocline because of the effect of the other factors. This procedure has been attempted without success in correlating the depth of the thermocline with sea and wind conditions alone.

On the other hand, on the basis of our present knowledge of the thermal structure, it can be shown that it would be just as hopeless to attempt to include all of the parameters in one relationship. This would amount, for all practical purposes to predicting the depth of the mixed layer for one particular time. Such a relationship might be written as follows:

$$D = \bar{D} + A_1 \sin \frac{2\pi t}{29 \times 24} + B_1 \cos \frac{2\pi t}{29 \times 24} + A_2 \sin \frac{\pi t}{12} + B_2 \cos \frac{\pi t}{12} + A_3 \sin \frac{\pi t}{6} + B_3 \cos \frac{\pi t}{6} + A_4 W \quad (19)$$

In this expression \bar{D} represents the seasonal effect, and may be taken as the mean depth of the thermocline for a particular month. The 2nd through 6th terms represent periodic effects due to the lunar, diurnal, and semidiurnal waves. In the last term, W is some function which represents the mixing processes that take place. It might be a complicated function of wind and sea, and only experiments will determine its exact nature. The contribution to the amplitude of the oscillations of the thermocline made by the lunar wave would be represented by $\sqrt{A_1^2 + B_1^2}$ and the phase change from the lunar at the thermocline depth is given by $\tan^{-1} \frac{B_1}{A_1}$. The same relationships obtain for the semidiurnal and diurnal waves. The normal procedure in such a study would be to evaluate from known data the constants A_1, A_2, B_1, B_2 , etc., and to assume that these constants hold with time for that particular place. Assuming this to be so, one could, therefore, knowing \bar{D} and the other factors, evaluate D for a particular time.

There is no evidence that either the amplitudes or phases of the constituents waves are conservative with time. On the contrary, there is evidence to support the fact that both the amplitudes and phases vary with time and also with depth at one particular time. Another difficulty lies in the nature of the function of the wind which must be used to evaluate turbulent

mixing. In the light of these facts, it would seem that, based on our present knowledge of the present processes involved, a precise empirical prediction of the thermocline depth is not now possible.

However, it is possible to make approximations. One of the things that we know about the diurnal and semidiurnal oscillations is that their amplitudes are dependent to a large extent on the depth at which these oscillations occur. For approximation purposes, therefore, the problem may be divided into two parts: (a) to predict the mean depth about which the thermocline oscillates daily and (b) to predict the amplitude of the oscillations about this depth.

The first of these is partly seasonal, partly random, and may be partly monthly. The problem involved is essentially one of extrapolating the curve shown in figure 19. Attempts have been made to devise a successful technique based on such parameters as persistency, surface temperatures, sharpness of the thermocline, and a departure of the depth of the thermocline from normal. As yet a relationship which can be considered sufficiently accurate has not been devised, but work on a successful method of approximation will be continued in the near future.

The second problem mentioned above has been attacked with some success. First, at several locations in the oceans at which many time-series BT observations were available, the mean amplitudes of the semidiurnal and diurnal oscillations were computed for each of several categories of depth at which the thermocline was found. The results are shown

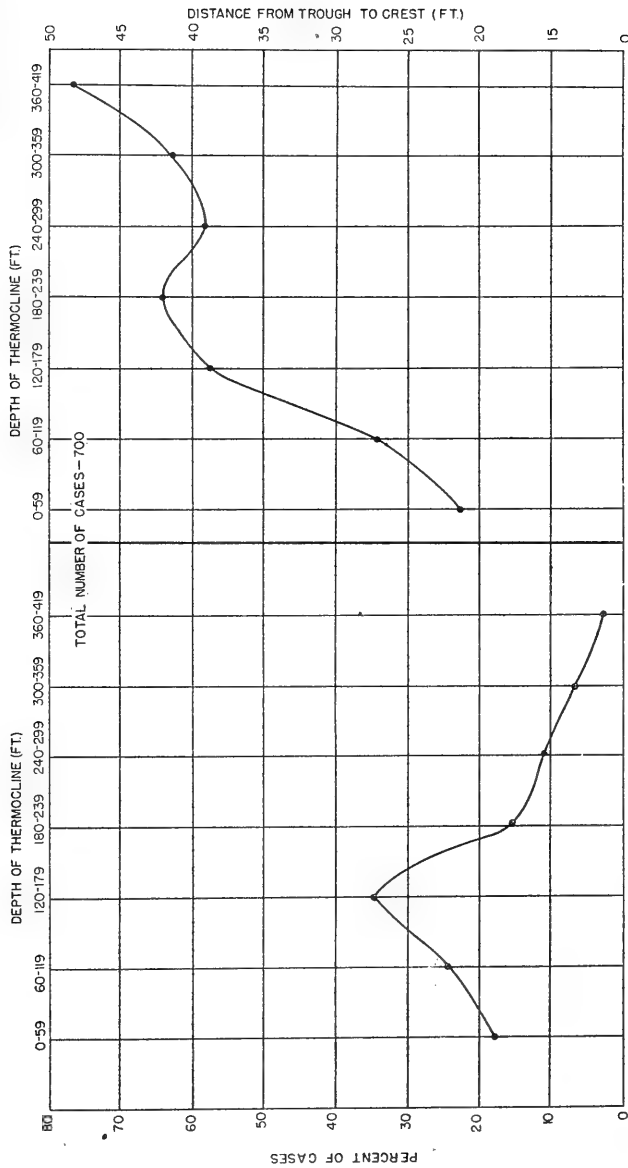


FIGURE 24A. PERCENTAGE DISTRIBUTION OF MEAN DAILY THERMOCLINE DEPTHS. B. RELATIONSHIP BETWEEN THE AMPLITUDE OF THE TIDAL INTERNAL WAVES AND THE MEAN DEPTH ABOUT WHICH IT OSCILLATES. PACIFIC WEATHER SHIP NECTAR, 30°N, 140°W, AND VICINITY

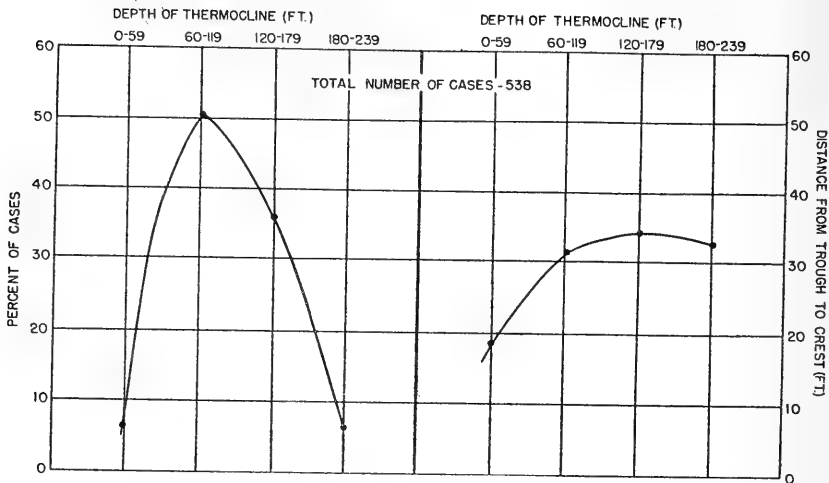


FIGURE 25A. PERCENTAGE DISTRIBUTION OF MEAN DAILY THERMOCLINE DEPTHS.

B. RELATIONSHIP BETWEEN THE AMPLITUDE OF THE TIDAL INTERNAL WAVE AND THE MEAN DEPTH ABOUT WHICH IT OSCILLATES.

ATLANTIC WEATHER SHIP COCA, 52.5°N, 35.5°W, AND VICINITY

in figures 24 and 25. In each figure the graph at the left indicates the percentage of the total observations which showed the mean depth of the thermocline at each of the depth categories and the graph at the right indicates the mean amplitudes plotted against each of the depth categories. It is evident that there is a direct relationship between the mean depth about which the thermocline is oscillating and the amplitude of the oscillations themselves. It will be noted that variations from a straight line relationship exist. In particular it was noticed that the slight decrease in the amplitude at the greater depths shown in the right-hand graph of figure 25 was also characteristic of some of the data computed for other areas of the ocean but not presented in this report. It is not known at present whether this is due to the relatively few observations taken where the thermocline was found at the greater depths or whether there is

some physical reason as yet unknown. In general, however, all areas in the ocean showed an increase in amplitude with an increase of the mean depth of the thermocline, which agrees substantially with the two-layer theory.

Such depth versus amplitude data may be used to devise an empirical relationship which will be applicable to one particular place in the ocean. As mentioned before, appendix A presents a derivation of an expression for the amplitude of a wave along the interface between two fluids using the linear two-layer theory and taking into account both the rotation and the spherical nature of the earth. This amplitude was found to be

$$\zeta_1 = \frac{\frac{K\Omega}{R \cos \phi} \left[\frac{AR \cos \phi}{h_I} + \frac{\sigma g \rho_I F'}{R \lambda \rho_{II} F} + \frac{Kg \rho_I F' A}{\lambda R \sigma \rho_{II} F} - \frac{Kg \rho_I}{R \rho_{II} \cos \phi} \right]}{\frac{A^2 R^2 \cos \phi}{h_I h_{II}} - \frac{AR \cos \phi}{h_I} \left(\frac{Kg \rho_I F' A}{\lambda R \sigma \rho_{II} F} + \frac{\sigma g \rho_I F'}{R \lambda \rho_{II} F} - \frac{Kg \rho_I}{R \rho_{II} \cos \phi} \right)} \quad (20)$$

The nature of the terms is explained in appendix A. It will be seen that many of the terms are functions of the latitude, radius of the earth, and the wave length. If we may assume, as Haurwitz did, a constant wave length for the semidiurnal and diurnal waves, then all of these terms become constant for a particular place. In addition, for deep water it is not possible for h_{II} to change very much relative to h_I , since it is so much greater in magnitude. Since ρ_{II} for all practical purposes may be considered constant, it is then possible to include both the depth and density of the lower layer in the constant terms.

By grouping the constants for each term together, the expression then becomes

$$\zeta_1 = \frac{\frac{K_1}{h_I} + K_2 + K_3 \rho_I}{\frac{K_4}{h_I} + K_5 \frac{\rho_I}{h_I}} \quad (21)$$

Here the K s are arbitrary constants to be determined. Rearranging terms and grouping the constants once again, we have

$$C_1 \zeta_1 + C_2 \rho_I \zeta_1 + C_3 h_I + C_4 \rho_I h_I = 1 \quad (22)$$

The expression is now in a form which may be subjected to a curve fitting procedure. From analyzed BT data for a particular area, such as is presented in figures 15 and 16, the amplitude and the depth of the thermocline h_I may be determined, and a good approximation of ρ_I may be arrived at from the surface conditions. By using sufficient data, the constants in equation (18) may be computed. This was done for the data available in the vicinity of the Pacific weather ship NECTAR (the data from this area are summarized in figure 24). When the constants were evaluated and the resulting expression solved for the amplitude, the following empirical relationship was obtained

$$2\zeta_1 = \frac{1-97.443 h_I + 95.0908 \rho_I h_I}{-280.0824 + 273.3448 \rho_I} \quad (23)$$

It was more convenient in processing these data to use the distance from trough to crest, rather than one-half distance. Therefore, in this expression $2\zeta_1$ represents not the actual

amplitude but twice that value.

This equation for the present should be considered a rough approximation only, since the actual data were so scarce and so infrequent that a true approximation of a continuous curve was not very often obtained. In order to test the equation, a few observations were available from weather ship NECTAR other than those used in computing the constants. A listing of the computed and observed heights (twice amplitude) follows:

<u>Computed</u>	<u>Observed</u>
28	26
21	15
38	36
32	27
105	48
93	82

The correlation coefficient between the above computed and observed heights is 0.69, which, for only six cases, is of no statistical significance. The results, however, seem to indicate a reasonable basis for further work on this type of approach. The information contained in equation (23) may be summarized by a single nomogram, as shown in figure 26. For a given density of the upper layer and for a given mean depth of the thermocline, the amplitude of the wave along the thermocline may be read off. An unusual feature of this equation is the fact that there exists a thermocline depth where the amplitude is independent of density, and remains nearly constant. No particular physical interpretation of this feature can be given. It should be emphasized once again that equation (23) and figure 26 are

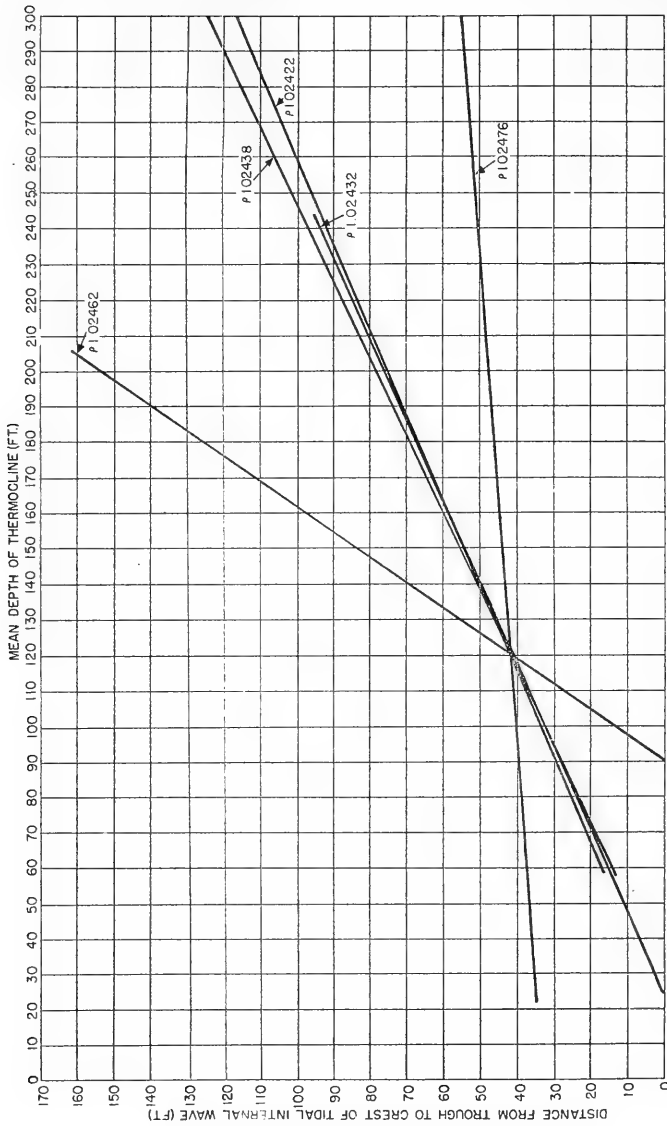


FIGURE 26. DISTANCE FROM TROUGH TO CREST OF THE TIDAL INTERNAL WAVE AS A FUNCTION OF THE MEAN DEPTH OF THE THERMOCLINE AND VARIOUS SURFACE DENSITIES. VICINITY PACIFIC WEATHER SHIP NEGTAR, 30°N, 140°W.

based on data taken from one location; therefore, they are valid only in that area.

3. The continuous density model

So far the investigation has centered around a model in which the wave occurs along the interface between two homogeneous layers of water. If more than one interface are present, then several internal waves can result. Concerning this eventuality, the Oceans (1932) says "...the greater the number of boundary surfaces the greater the number of internal waves. On the basis of this reasoning, when the density varies continuously with depth one should expect an unlimited number of possible internal waves." The effect of this concept upon an investigation of periodic variations in the oceans frequently would be to give results different in nature from those given by the two-layer system. With many infinitesimal vertical changes in density occurring simultaneously, it does not necessarily follow that the largest amplitude will be found at the thermocline. A complete statistical analysis of this problem has been presented by Seiwel (1942). This consists of a complete harmonic analysis of the oscillations at several depths at "Atlantis" anchor station 3245. One of the main conclusions of this work was that the smaller the vertical density gradients at a given depth, the larger will be the amplitudes of the oscillations, and the smaller will be the temperature changes with time at that depth. In the case of the particular data that were analyzed in this study, it was found that the greatest amplitudes occurred at a depth somewhat greater than that of

the thermocline.

The picture thus presented by the continuous density model is one much more complicated in nature than that of the two-layer system. We are now concerned with an ocean in which the amplitudes and phases of the internal wave are continuous functions of depth.

The most complete theoretical treatment of this complicated problem has been given by Fjeldstad (1933). Assuming free waves in a medium in which density varies continuously with depth and neglecting the effect of friction, Fjeldstad derives the following second order differential equation

$$\frac{d^2 w}{dz^2} + \lambda^2 g \phi w = 0 \quad (24)$$

with boundary conditions at the bottom ($w=0$, $Z=0$)

and at the surface ($w=0$, $Z=h$).

In this equation, w represents the relative displacement of a water particle from its equilibrium position. This means that these amplitudes are not unique, but only that they are determined in such a way that the ratio of true amplitudes between any two fixed depths is equal to the ratio of the w 's for the same depth. The term ϕ is taken as the internal stability of the water column, or

$$\phi = \frac{1}{\rho} \frac{d\rho}{dz} \quad (25)$$

$\lambda^2 g$ is an unknown parameter which depends on the vertical density distribution.

It is necessary in general to carry out this integration by numerical methods, and an infinite number of solutions corresponding to an infinite number of internal waves are possible. This integration yields the solution for the relative amplitudes w .

The internal wave motion is then assumed to be of the following form

$$\eta = A \cos \sigma t + B \sin \sigma t \quad (26)$$

Where the computed amplitudes may be evaluated by the following summations

$$A = \sum_{n=1}^{\infty} a_n w_n \quad B = \sum_{n=1}^{\infty} b_n w_n \quad (27 \text{ a,b})$$

The coefficients a_n and b_n may be evaluated by the use of the Fourier theorem

$$a_n = k \int_0^h A \phi(z) w_n dz \quad b_n = k \int_0^h B \phi(z) w_n dz \quad (28 \text{ a,b})$$

It will be noted that in computing the Fourier coefficients a_n and b_n it is necessary to have observed amplitudes A and B in equations (28). These coefficients are then used to compute the actual amplitudes in equations (27). No matter what the nature of the orthogonal function w , the Fourier theorem requires that the observed and computed amplitudes must be identical, if an infinite number of orders are used. However, Fjeldstad demonstrates that, by employing his particular w , good agreement is

obtained between the observed and computed amplitude in four orders. This is a very strong mathematical indication of the validity of his theoretical formulation. His differential equation, therefore, has been widely employed in studies by other authors, notably Seiwell (1942) and Lek (1938).

It must be emphasized that Fjeldstad was concerned primarily with validating his theory, and not with computing amplitudes at a time and in a place where no amplitudes were known. His work has been examined in the present investigation with a view to projecting his results into the future in order to predict the character of the semidiurnal and diurnal internal wave in a given place at some future time. It was hoped that in his concepts could be found some conservative or predictable factor which could be employed in a technique for successful prediction.

The most convenient and appealing idea was that the Fourier coefficients themselves were conservative with time for any one place. However, no satisfactory theoretical defense for this thesis could be found, since it seems clear from the above equations that, if the density distribution changes with time, not only would the amplitude A change but also the coefficients a_n . This does not mean, however, that this concept as a possible basis for a prediction technique should be discarded entirely. In cases of slow time rate of change of density distribution, it is possible that the coefficients would remain reasonably constant with time; from a practical standpoint this would be almost as useful as absolute constancy. It may be that even for large

density changes with time there would not be much change in the coefficients, but this has not as yet been shown. However, Pekeris (1937) and Wilkes (1949) have investigated a similar problem in the atmosphere, with the difference that they postulate a driving force rather than assume free waves. An examination of their work reveals the hope that a similar treatment of the oceans will show that the Fourier coefficients will remain relatively conservative with time, since analogous terms in the work of Pekeris depend only on the vertical density distribution and the location.

Since the approximate conservativeness of the Fourier coefficients could not be demonstrated, it was decided to proceed upon the assumption that a change in these values occurs. It was further assumed that when this change occurred, it occurred in such a manner that the change in the time components of the semidiurnal and diurnal waves was a minimum. This assumption was predicated on the concept that, for any new set of initial conditions, the ocean like all fluids will reach equilibrium with these new conditions with the least possible change in the motion.

Many possibilities for minimizing changes other than the above present themselves. For instance, one could attack the problem of minimizing the change in energy from one set of conditions to another by minimizing the change in the square of the amplitude. Another possibility would be to attempt to minimize the change in the amplitudes and the phases themselves. While these techniques obviously have merit, they were super-

ficially investigated and found to require a computational treatment far longer than the limited staff of the project could supply. With the aid of machine computation, however, this problem could be attacked in the future. Therefore, it was decided to proceed with the original assumption.

Let A_1 be one of the two constituents of the amplitude of a wave computed from the observed data at one particular time according to Fjeldstad's theory. Let A_2 be the corresponding unknown component for some future time at the same place. At this future time, let one observation of vertical density distribution be available so that the w 's are known.

$$\text{Let } \sum_{n=1}^4 (a_{1n} w_{1n} - a_{2n} w_{2n})^2 = I(a_{2n})$$

$$n=1,2,\dots,4 \quad (29)$$

Now by minimizing the function I we are minimizing the change of the component of the amplitude of the wave A_1 (see equation 27). The minimizing of the function I may be accomplished by the solution of four simultaneous equations which will yield the unknown a_{2n} . This computation is long and involved and, for the example mentioned below, will not be repeated here. It was carried out by desk calculator by using the inverse matrix approach. For the harmonic analysis and the numerical integration, techniques identical with those of Fjeldstad were employed.

The type of data required to test this method is that obtained at a standard anchor station of at least 24 hours' dura-

tion, repeated at some future time in exactly the same place. Adequate data such as these are not as yet available. The only repeated anchor station the investigators could find in all literature was that taken in the Florida Straits by two U. S. Navy Hydrographic Office Survey ships, the SAN PABLO and the REHOBOTH, on the 4th and 9th of December 1950. The deficiencies of these data were many, and they will be discussed later. However, since these were the only data available, it was decided to employ them, more as an instrument for developing a technique than as an honest test of the method.

The data for 4 December were analyzed according to Fjeldstad's method and the values for the Fourier coefficients are presented in table VIII. By numerical integration the relative amplitudes, w , were computed for the 4 December data at 5 chosen depths. These values are given in table IX. The data for 9 December were analyzed in the same manner and the relative amplitudes are presented in table X.

Table VIII

Order	Diurnal	Semidiurnal
a_1	.949	.252
a_2	- .980	.160
a_3	- .951	-1.019
a_4	- .848	2.830

Fourier coefficients as computed from anchor station of 4 December 1950.

Table IX

Depth (meters)	w_1	w_2	w_3	w_4
50	4.90	4.57	3.99	3.32
75	6.99	5.19	2.58	0.34
100	8.20	2.58	-1.27	-1.05
125	7.61	-3.06	-1.35	1.53
150	6.04	-6.50	1.10	-0.01

Relative amplitudes, w , as computed from anchor station of 4 December 1950.

Table X

Depth (meters)	w_1	w_2	w_3	w_4
50	4.87	4.25	3.36	2.22
75	6.91	4.38	1.55	- 0.68
100	7.86	1.05	-1.92	- 0.47
125	7.25	-3.28	-0.90	1.27
150	5.79	-5.45	1.51	0.02

Relative amplitudes, w , as computed from single density distribution on 9 December 1950.

Table XI

Order	Diurnal	Semidiurnal
a_1	-.016	-1.114
a_2	.112	1.049
a_3	-1.210	1.058
a_4	1.813	-.843

Predicted Fourier coefficients
for 9 December 1950

Table XII

Depth (meters)	A_1 Predicted	A_1 Observed
50	-6.44	-10.00
75	-1.19	6.60
100	7.35	4.90
125	10.20	11.60
150	11.05	10.60

Predicted and observed absolute amplitudes
(meters) of the diurnal internal wave on
9 December 1950

The data presented in tables VIII, IX, and X may now be inserted in equations (29) and the solutions for the predicted Fourier coefficients on the 9th of June obtained. These are given in table XI. By using these predicted Fourier coeffi-

cients, the data for the relative amplitudes for the 9th of December given in table X, and equation (27a), it is now possible to predict one of the components of the internal wave for the 9th of December. The values of this component for each of the chosen depths are given in table XII. Finally, as a verification, it was necessary to compute by harmonic analysis the actual observed components of the amplitudes. These observed amplitudes are also shown in table XII. In like manner it is possible to compute the other component of the amplitude.

A comparison of the predicted and observed amplitudes as given in table XII indicates that the results, while promising, are not entirely satisfactory. In general, it is considered that there are two main reasons for the discrepancies in the forecast. First, there are deficiencies in the data themselves. The anchor stations on the 4th and 9th of December were each taken by two ships anchored approximately 30 miles apart. Each ship took 6 observations during the 24-hour period of the 4th and these were combined to form one set of 12 observations for that one day. The procedure was repeated on the 9th. The fact that the ships were anchored so far apart undoubtedly introduced reasonably large errors in the harmonic analyses. Furthermore, the anchor stations were located in shallow water and in an area in which reasonably strong currents exist. All these factors tended to contaminate the results. Second, there is a possibility that the incorrect parameter was minimized. This has already been discussed. In the future it is planned to conduct other trials minimizing other parameters.

Another interesting feature of these results is the fact that the prediction was much more accurate at greater depths than at the surface. The example shown in table XII includes only one component of the diurnal wave; actually both components for both the semidiurnal and diurnal wave were computed. In all four cases the results displayed the same inaccuracy near the surface and the same accuracy at the greater depths. Whether this particular inaccuracy is due either to one of the above two reasons or to some near-surface phenomenon not considered in the computations has not as yet been determined.

It will be noted that the technique outlined above does not, according to strict terminology, constitute a true forecast, since either an observation or an assumption of a present density distribution is necessary to employ the method. However, it is considered a large step forward to be able to estimate the amplitude of the wave from a single observation, rather than from a complete anchor station with many time-series observations. If some such method as described above were to be developed, it would automatically increase the chances of predicting the internal wave, for it is not possible to occupy a complete anchor station every time a forecast is desired. If one harmonically analyzed all existing and future anchor stations and computed the Fourier coefficients for each, then at any future time the internal wave could be estimated for each of these areas. The only data one will need for this operation would be a single density distribution. This observation could be either (a) a recent observation taken in the area, (b) an estimated distri-

bution based on the latest available data and extrapolation, or (c) a predicted distribution based on climatological data for the particular month desired and tempered by the latest information and by experience. It is believed that, if a mass of data as mentioned above was collected and such a technique developed, it would be of great value in delineating one of the main effects upon the thermal structure of the ocean. With this effect evaluated, it would then be possible to proceed to the study of other factors.

III. Data

The single feature that has had the greatest effect on the course of this investigation has been the lack of data suitable for conducting it. When the approach to be employed in this investigation was first decided upon, the type of data that would be necessary to employ this approach immediately became clear. It was evident that most of the data that were available from various sources had two serious defects: (a) The data were obtained by the classical technique; that is, both time and distance were allowed to vary in obtaining the serial observations, and (b) none of the data contained measurements of a sufficient number of parameters to evaluate completely all the effects on the thermal structure.

The first of these defects is by far the more important. It is the opinion of the investigators that, if problems such as this are to be solved eventually, more attention must be given to eliminating the factor either of time or distance from the collection of data. One of the first things that becomes evi-

dent in recent oceanographic literature is that, when analyses are made either of time-series or synoptic data, the ocean is found to be much less invariant with time than was heretofore assumed. No better illustration of this thesis could be given than that of Defant (1950) who demonstrated that, when one eliminates the effect of each observation being taken at a time and place different from every other observation, an entirely different and more credible pattern of the oceanographic variables results. In this case Defant eliminated the effect of the tidal internal wave, but undoubtedly a thorough investigation of other factors, such as the effect of horizontal gradients in the ocean, would give the same result.

It was clear that what was needed for this investigation was a series of repeated anchor stations taken at one or more locations. These anchor stations initially should be in locations where the variables which could not be accurately measured would have little or no effect, such as an area where relatively little current exists and where there are no abrupt changes in bottom topography. These observations should be repeated every hour or two, and frequent BT's taken at regular intervals. They should also include simultaneous observations of such other parameters as might be important to changes in the thermal structure, such as incoming and outgoing radiation, transparency, air temperature and humidity, wind, and sea and swell. It was considered that not too much could be learned from single anchor stations of one day's duration since they afford little or no opportunity for testing techniques or

conclusions.

The alternative to anchor station type of data would be a series of observations taken simultaneously by several ships each at a different location. This type of synoptic data would be very useful if one wished to consider the effects of horizontal advection on the thermal structure, since it would give an estimation of horizontal gradients. Actually the optimum would be a combination of the two types of data. Except for the possibility of expanding the weather ship program, however, the cost of any such network as a regular procedure would be prohibitive.

This then was the type of data that was desired. Searches were made in all possible sources in order to obtain the data which best fit the requirements, but with very little success. By far, the bulk of the time-series data available consists of BT data taken from weather ships. In addition the only repeated anchor stations that could be found were the set of observations used in the example in the text. The deficiencies of both these types of data have been discussed above in connection with the discussion of the use to which the data was put.

Although the data acquired in time to be of use in this report were far from adequate, much progress has been made both in arranging for complete collections of suitable data and in the development of new observational techniques aimed at increasing the value of the data. Much of this work has been carried on in the Hydrographic Office itself. Arrangements have been made for future cruises of the Hydrographic Office survey ships

to include among their observations long term anchor stations in suitable locations with closely spaced serial observations of all measurable parameters. One of these cruises, AMOS XI, is now in progress and the data will be available in the very near future. In addition, in cooperation with the Office of Naval Research, plans have been completed for conducting a series of cruises of five days' duration in each month to collect similar data to be utilized synoptically with the observations taken at weather ship HOTEL. The U. S. Navy Hydrographic Office has been very active in improving the instrumentation required for this type of oceanographic data. The radiation data presented in the first section of this report constitutes one of the first sets of data from a recently developed pyr heliometer array now installed on the U. S. Navy Hydrographic Office Survey ship REHO-BOTH. New photometric equipment is now being tested with a view to improving methods of obtaining transparency data with depth. In addition, the Hydrographic Office has developed to a stage of near completion a thermopile to supplement BT observations which is expected to yield much valuable information on the microthermal structure of the ocean. This device is of great interest to the present investigators, not only because of its obvious value in estimating very small changes in the thermal structure due to processes such as radiation and evaporation, but also because of its great possibilities as an instrument for measuring fluctuations in temperature of a periodic nature. Such an instrument, when held at a constant depth, would give a good indication of these periodic fluctuations; several such units, each at a dif-

ferent depth, would delineate the relationship between amplitude and phases at these different depths.

IV. Recommendations for future work

The project as it has developed so far has opened several avenues of approach which, if followed, should yield interesting and useful results of a practical nature. These consist partly of extending approaches already employed by utilizing more adequate data, and partly new approaches suggested by various phases of the work and by the literature. They may be summarized as follows:

a. A re-evaluation should be made of the first portion of this study dealing with the direct effect of meteorological parameters, such as radiation, evaporation, and wind. It seems clear that the small changes in the thermal structure caused by changes in these parameters must have an important effect on operational problems connected with sound. It is believed that with increased accuracy of the instruments discussed above, especially those such as the thermopile dealing with the measurement of temperature, much useful information may be obtained.

b. It is planned to continue and expand the effort to arrive at useful empirical relationships aimed at predicting the mixed layer depth.

c. Further computations using the continuous density model of Fjeldstad are proposed, by utilizing more accurate data and making such revisions of the technique as necessary.

d. It is also planned to investigate the possibility of attacking the problem of tidal oscillations in a direct manner,

i.e., by considering the tidal force itself. This would be a purely deductive method stemming directly from the differential equation.

e. Another possible approach now being considered is an attempt to develop a purely noncausal technique of predicting the thermal structure by using the principles of statistical mechanics. This would probably employ the largest possible collection of BT time-series data and would be developed by using standard techniques of time-series prediction. In such a study it would be necessary to assume some particular statistical form of the distribution of the components of the periodic oscillations. An interesting treatment of this type was applied by Pierson (1952) who demonstrated prediction in time and space of a wave train whose displacements from the mean displayed a Gaussian distribution.

f. All the BT data at the Hydrographic Office are now being analyzed for the occurrence of synoptic situations, or situations in which there was a reasonably large horizontal distribution of observations for a given period of time. If good examples of such distributions are found, it is intended to attempt to apply well-known techniques of extrapolation and kinematic analysis, with a view to developing a useful prediction tool.

APPENDIX A

Consider a two-layer system in which the upper layer has a density of ρ_I and a depth of h_I , and the lower layer has a density of ρ_{II} and a depth of h_{II} .

Let U and V be the east-west and north-south components of velocity, respectively, and let ζ_0 and ζ_1 be the displacements from their equilibrium positions of the ocean surface and the internal boundary, respectively. The equation of horizontal motion in the north-south directions is

$$\frac{\partial V}{\partial t} - \lambda U = -\frac{1}{R} \frac{\partial}{\partial \phi} \left(\frac{P}{\rho} + gz + \Omega + \frac{1}{2} \omega^2 R^2 \sin^2 \phi \right) \quad (A1)$$

where ϕ = colatitude

R = radius of the earth

λ = the Coriolis parameter ($2\omega \sin \phi$)

ω = angular velocity of the earth

Ω = tidal potential

P = pressure

ρ = density

Allowing the subscript I to refer to the upper layer and the subscript II to refer to the lower layer, and making the following basic assumption,

$$\Omega, U_I, U_{II}, V_I, V_{II}, \zeta_0, \zeta_I, \sim AF(\phi)e^{i(K\theta - \sigma t)}$$

where $F(\phi)$ = some function of latitude

K = an integer

σ = the frequency of the tidal wave $\left(\frac{2\pi}{T} \right)$

we have, using the equation of continuity,

$$\frac{\partial V_I}{\partial t} - \lambda U_I = -\frac{1}{R} g \zeta_0 F' \quad (A2)$$

$$\frac{\partial V_{II}}{\partial t} - \lambda U_{II} = -\frac{1}{R} \left[g \frac{\rho_I F'}{\rho_{II} F} \zeta_0 + g \left(1 - \frac{\rho_I}{\rho_{II}} \right) \frac{F'}{F} \zeta_I \right] + \frac{1}{2} \omega^2 R \sin 2\phi \quad (A3)$$

By use of the original basic assumption, the divergence theorem for spherical coordinates may be applied, with the further assumption that the horizontal divergence

is independent of depth. Integrating with respect to depth from 0 to h_I and from h_I to $(h_I + h_{II})$, we obtain

$$\frac{\partial}{\partial t} (\zeta_0 - \zeta_I) = -h_I \left[\frac{1}{R \cos \phi} \left\{ V_I \left(\frac{F'}{F} \cos \phi - \sin \phi \right) \right\} + \frac{i k U_I}{R \cos \phi} \right] + \frac{1}{2} \omega^2 R \sin 2\phi \quad (A4)$$

$$\frac{\partial \zeta_I}{\partial t} = -h_{II} \left[\frac{1}{R \cos \phi} \left\{ V_{II} \left(\frac{F'}{F} \cos \phi - \sin \phi \right) \right\} + \frac{i k U_{II}}{R \cos \phi} \right] \quad (A5)$$

Now we may substitute the expression for U_I from equation (A2) to equation (A4).

$$\frac{\partial}{\partial t} (\zeta_0 - \zeta_I) = -h_I \left[\frac{1}{R \cos \phi} \left(\frac{F'}{F} V_I \cos \phi - V_I \sin \phi \right) + \frac{i k}{\lambda R \cos \phi} \left(\frac{\partial V_I}{\partial t} + \frac{1}{R} g \frac{F'}{F} \zeta_0 - \frac{1}{2} \omega^2 R \sin 2\phi \right) \right] \quad (A6)$$

This equation may be integrated with respect to t , as follows

$$\zeta_0 - \zeta_I = -\frac{h_I}{R \cos \phi} \left[\frac{i V_I}{\sigma} \left(\frac{F'}{F} \cos \phi - \sin \phi \right) + \frac{i k}{\lambda} \left(V_I + \frac{1}{\sigma R} g \frac{F'}{F} \zeta_0 - \frac{1}{2} \omega^2 t R \sin 2\phi \right) \right] \quad (A7)$$

and the resulting expression solved for V_I .

$$V_I = \left[\frac{R \cos \phi}{h_I} (\zeta_0 - \zeta_I) - \frac{K}{\lambda} \left(\frac{g}{\sigma R} \frac{F'}{F} \zeta_0 - \frac{1}{2} \omega^2 t R \sin 2\phi \right) \right] \frac{1}{\sigma} \frac{1}{\left(\frac{F'}{F} \cos \phi - \sin \phi \right) + i \lambda} \quad (A8)$$

If we solve equation (A2) for U_I ,

$$U_I = \frac{1}{\lambda} \left[\frac{1}{R} g \frac{F'}{F} \zeta_0 + \frac{1}{2} \omega^2 R \sin 2\phi - i \sigma V_I \right] \quad (A9)$$

we obtain two equations, (A8) and (A9), which give U_I and V_I in terms of ζ_0 and ζ_I only.

Now, to obtain the same type of expression for U_{II} and V_{II} it is necessary to integrate equation (A5).

$$\zeta_I = \frac{-h_{II}}{R \cos \phi} \left[\frac{i}{\sigma} V_{II} \left(\frac{F'}{F} \cos \phi - \sin \phi \right) + \frac{ik}{\lambda} \left\{ V_{II} + \frac{1}{R} \left(\frac{g_i}{\sigma} \frac{\rho_I}{\rho_{II}} \right) \frac{F'}{F} \zeta_0 + \frac{ig}{\sigma} \left\{ 1 - \frac{\rho_I}{\rho_{II}} \right\} \frac{F'}{F} \zeta_I + \frac{1}{2} \omega^2 + R^2 \sin 2\phi \right\} \right] \quad (A10)$$

solving equation (A10) for V_{II} ,

$$V_{II} = \left[\frac{R \zeta_I \cos \phi}{h_{II}} - \frac{K}{\lambda R} \right] \frac{F'}{F} \zeta_0 + \frac{g}{\sigma} \left(1 - \frac{\rho_I}{\rho_{II}} \right) \frac{F'}{F} \zeta_I + \frac{1}{2i} \omega^2 + R^2 \sin 2\phi \left\} \frac{1}{\sigma} \frac{1}{\left(\frac{F'}{F} \cos \phi - \sin \phi \right) + \frac{K}{i\lambda}} \right] \quad (A11)$$

and substituting this expression for V_{II} into equation (A3), we obtain

$$U_{II} = \frac{1}{\lambda} \left[-i \sigma V_{II} + \frac{1}{R} \left\{ g \frac{\rho_I}{\rho_{II}} \frac{F'}{F} \zeta_0 + g \left(1 - \frac{\rho_I}{\rho_{II}} \right) \frac{F'}{F} \zeta_I + \frac{1}{2} \omega^2 R^2 \sin 2\phi \right\} \right] \quad (A12)$$

If we substitute the expressions for U_I and V_I as given by equations (A8) and (A9) into (A7), and the expressions for U_{II} and V_{II} as given by equations (A11) and (A12) into (A10), we obtain two simultaneous equations in ζ_0 and ζ_I . Eliminating negligible terms, we obtain

$$\frac{\sigma^2 k \left(\lambda - \frac{\sigma^2}{\lambda} \right) \frac{R \cos \phi \zeta_0}{h_I} - \frac{AR \cos \phi}{\left(\frac{F'}{F} \cos \phi - \sin \phi \right)^2 + \frac{\sigma^2 k^2}{\lambda^2}} \zeta_I = \frac{-K\Omega}{R \cos \phi} \quad (A13)$$

$$\left[\frac{-\sigma g \rho_I F'}{R \lambda \rho_{II} F} - \frac{Kg \rho_I F' A}{\lambda R \sigma \rho_{II} F} + \frac{Kg \rho_I}{R \cos \phi \rho_{II}} \right] \zeta_0 + \left[\frac{-\sigma g \left(1 - \frac{\rho_I}{\rho_{II}} \right) F'}{R \lambda F} + \frac{R \cos \phi A}{h_{II}} + \frac{g \left(1 - \frac{\rho_I}{\rho_{II}} \right) F'}{F} A + \frac{Kg \left(1 - \frac{\rho_I}{\rho_{II}} \right)}{R \cos \phi} \right] \zeta_I = \frac{-K\Omega}{R \cos \phi} \quad (A14)$$

Solving these equations simultaneously, we arrive at the desired expression for ζ_I .

$$\zeta_I = \frac{\frac{K\Omega}{R \cos \phi} \left[\frac{AR \cos \phi}{h_I} + \frac{\sigma g \rho_I F'}{R \lambda \rho_{II} F} + \frac{Kg \rho_I F' A}{\lambda R \sigma \rho_{II} F} - \frac{Kg \rho_I}{R \cos \phi \rho_{II}} \right]}{\frac{A^2 \cos^2 \phi}{h_I h_{II}} - \frac{h_I}{\lambda R \sigma \rho_{II} F} \left(\frac{Kg \rho_I F' A}{R \cos \phi A} + \frac{\sigma g \rho_I F'}{R \lambda \rho_{II} F} - \frac{Kg \rho_I}{R \cos \phi \rho_{II}} \right)} \quad (A15)$$

BIBLIOGRAPHY

- ANGSTROM, A. 1920. Application of heat radiation measurements to the problems of the evaporation from lakes and the heat convection at their surfaces. Geogr. Ann., Heft III, 16 pages, 1920.
- 1922. Note on the relation between time of sunshine and cloudiness in Stockholm, 1908-1920. Arkiv fur matematik, Astronomi och Fisik, Band 17, No. 15, Stockholm, 1920.
- DAVIES, T.V. 1951. Finite amplitude gravity waves. Symposium on Gravity Waves, National Bureau of Standards, 1951 (unpublished).
- DEFANT, A. 1932. Die Gezeiten and inneren Gezeitenwellen des Atlantischen Ozeans. Deutsche Atlantische Exped. Meteor 1925-27, Wiss. Erg., Bd. 7, Heft I, 313 pp. 1932.
- 1949. Convection and ice potential in the polar shelf seas. Geogr. Ann., Heft XXXI, pp. 25-35, 1949.
- 1950. Reality and illusion in oceanographic surveys. Jour. Mar. Res., v. IX, no. 2 pp. 120-138, 1950. (SIO contribution new series no. 478).
- EKMAN, V.W. 1904. On dead water. Norwegian north polar expedition, 1893-1896, sci. results, v. 5 no. 15, 152 pp. 1904.
- 1928. A survey of some theoretical investigations of ocean currents. Jour. du conseil, v. 3 no. 3 pp 295-327, 1928.
- FJELDSTAD, J. E. 1933. Interne Wellen, Geofysiske Publikasjoner, v. 10, no. 6. 53 pp. 1933.
- HAURWITZ, B. 1950. Internal waves of tidal character. Trans. AGU, v. 31, no. 1, 1950 (WHOI contribution no. 477).
- , and J. M. AUSTIN. 1944. Climatology. New York. McGraw-Hill. 410 pp. 1944.
- HELLAND-HANSEN, B., and F. NANSEN. 1909. The Norwegian Sea. Norwegian Fishery and Marine Investigations Report, v. 2 pt. 1, no. 2, 390 pp. plus tables, 1909.

- JACOBS, W.C. 1942. On the energy exchange between sea and atmosphere. *Journal Mar. Res.*, v. 5, no. 1, pp. 37-66, 1942.
- KIMBALL, H. 1928. Amount of solar radiation that reaches the surface of the earth on the land and on the sea. *Mo. Wea. Rev.*, vol. 56 No. 10, pp, 393-398, 1928.
- LAMB, Sir H. 1932. *Hydrodynamics*. London. Cambridge University Press. 6th ed., 738 pp. 1932.
- LEK, L. 1938. Die Ergebnisse der Strom-und Serienmessungen. Snellius Exped. in the eastern part of the Netherlands East-Indies, 1929-1930, v. 2, pt. 3, 169 pp. 1938.
- MOSBY, H. 1936. Verdunstung und Strahlung auf dem Meere. *Ann. der Hydrog. u. Marit. Meteor.* Vol. 54, pp. 281-286, 1936.
- MUNK, W. H. 1947. A critical wind speed for air-sea boundary surfaces. *Jour. Mar. Res.* v6., no. 3, pp. 203-218, 1947.
- MUNK, W. H., and E. R. ANDERSON, 1948. Notes on a theory of the thermocline. *Jour. Mar. Res.* v. 7, no. 3, pp. 276-295, 1948 (SIO contribution new series no. 382).
- PEKERIS, C. L. 1937. Atmospheric oscillations. *Proc. of the Roy. Soc. series A*, v. 158, pp. 650-671, 1937.
- PETTERSSEN, S. 1940. *Weather Analysis and Forecasting*. N.Y. McGraw-Hill. 505 pp. 1940.
- PIERSON, W. J. Jr. 1952. A unified mathematical theory for the analyses, propogation, and refraction of storm generated ocean surface waves, Part I. *Pub. N.Y. Univ. Coll. of Eng., Dept of Meteorology*, 336 pp., 1952.
- SANDSTROM, J. W. 1914-15. The hydrodynamics of Canadian Atlantic Waters. *Canadian Fisheries Exp.* 1914-15, 292 pp., 1914-15.
- SCHMIDT, W. 1915. Strahlung und Verdunstung an freien Wasserflachen. *Ann. der Hydrog. u. Marit. Meteor.*, Vol. 3 and 4, 1915.
- SEIWELL, H. R. 1939. The effect of short period variations of temperature and salinity on calculations in dynamic oceanography. *Papers in Phys. Ocean. and Met.*, published by MIT and WHOI, v. 7, no. 3, 32pp. 1939

- 1942. An analysis of vertical oscillations in the southern North Atlantic. Proc. Am. Phil. Soc. v. 85, no. 2, 1942 (WHOI contribution no. 291).
- 1949. The principles of time series analysis applied to ocean wave data. Proc. Nat. Acad. of Sci., v. 35, no. 9, pp. 518-528, 1949.
- SVERDRUP, H. U., M. W. JOHNSON, and R.H. FLEMING. 1942. The Oceans. N. Y. Prentice Hall, Inc., 1087 pp. 1942.
- TAYLOR, G. I. 1936. The oscillations of the atmosphere. Proc. of the Royal Soc. of London., series A, v. 156, pp. 318-326, 1936.
- UFFORD, C. W. 1947. Internal waves in the ocean. Trans. AGU, v. 28, no. 1, pp. 79-86, 1947.
- 1947 b. Internal waves measured at three stations. Trans. AGU, v. 28, no. 1, pp 87-95, 1947.
- 1947 c. The theory of internal waves. Trans. AGU, v. 28, no. 1, pp 96-101, 1947.
- WEINER, N. 1949. Extrapolation, Interpolation, and Smoothing of Stationary Time Series. N. Y. Technology Press of MIT and Wiley and Sons, Inc., 163 pp. 1949.
- WILKES, M. 1949. Oscillations of the Earths Atmosphere. Cambridge Monographs on Physics. Cambridge. 74 pp. 1949.
- ZEILON, N. 1911. On tidal boundary waves. Kungl. Svenska Vetenskapsakademiens Handlingar. v. 47, no. 4, 46 pp. 1911.
- ZUBOV, N. N. 1938. Morskije Vody i l'dy. (Marine Water and Ice). Moskva, Gidrometeoizdat, 451 pp. 1938.



